

10. NONDESTRUCTIVE EVALUATION

A. Nondestructive Inspection of Adhesive Metal-Metal Bonds (NDE601*)

Principal Investigators: David G. Moore
Sandia National Laboratories
P.O. Box 5800, MS 0863
Albuquerque, NM 87185
(505) 844-7095; e-mail: dgmoore@sandia.gov

Dennis Roach
Sandia National Laboratories
P.O. Box 5800, MS 0615
Albuquerque, NM 87185
(505) 844-6078; e-mail: dproach@sandia.gov

Ciji L. Nelson
Sandia National Laboratories
P.O. Box 5800, MS 0615
Albuquerque, NM 87185
(505) 843-8722; e-mail: cijnels@sandia.gov

Cameron J. Dasch
General Motors Research & Development
30500 Mound Road, Warren, MI 48090
(586) 986-0588; fax: (586) 986-3091; e-mail: cameron.j.dasch@gm.com

Technology Area Development Manager: Joseph A. Carpenter
(202) 586-1022; fax: (202) 586-1600; e-mail: joseph.carpenter@ee.doe.gov

Field Project Officer: Aaron D. Yocum
(304) 285-4852; fax: (304) 285-4403; e-mail: aaron.yocum@netl.doe.gov

Contractor: U.S. Automotive Materials Partnership (USAMP)
Contract No.: DE-FC26-02OR22910

Objective

- Identify and develop one or more nondestructive inspection (NDI) methods for adhesive bond evaluation to be used in an automotive manufacturing environment that would foster increased confidence and use in adhesive joining. The wider use of adhesive joining could result in reduced vehicle weight, increased body stiffness, and improved crashworthiness. Adhesives are also seen as a critical enabler for the joining of dissimilar materials in order to avoid corrosion from dissimilar metals.
 - To accomplish this goal, the various attributes that determine the bond strength must be identified along with an NDI method to measure that property. The success of this approach will be quantitative correlations of NDI to measured bond strengths.

* Denotes Project 601 of the Nondestructive Evaluation (NDE) Working Group of the United States Automotive Materials Partnership, one of the formal consortia of the United States Council for Automotive Research set up by Chrysler, Ford, and General Motors to conduct joint, precompetitive research and development (see www.uscar.org).

- The target methods must be able to perform the inspection on the plant floor in at least an off-line audit time window and be able to inspect most of the adhesive bonds on current production vehicles.

Approach

- There are five major attributes that contribute to the strength of an adhesive bond on a metal flange: the width of the adhesive area, the adhesive thickness, the location of the bead relative to the edges of the flange, the state of cure, and the quality of the adhesion. The general approach is to develop inspection techniques that can be used on the manufacturing floor which allow all the required adhesive characteristics to be measured nondestructively.
- The chosen methods must be single-side inspections that can follow a flange, navigate large changes in geometry, have spatial resolution near 1 millimeter (mm) and have an overall inspection speed of at least 1 meter per minute (m/min).
- To accomplish this, there is a two step validation process: first, successfully inspect the flat adhesively bonded specimens, representative of automobile flanges. This includes comparison to measurements of the bond strength. Second, deploy the inspection method on production car bodies.
- The flat specimens vary in adhesive, adherent type and thickness, stackup (2–3 layers), cure state, and surface contaminants. These conditions bound the processing parameters for the adhesive assembly process. A through-transmission ultrasonic inspection is performed to characterize the flat specimens and is considered a “gold standard” reference inspection method. Selected samples are also peel tested to measure bond strengths.
- Multiple automotive bodies-in-white (BIW) containing many adhesive joints were produced by the Original Equipment Manufacturers (OEMs) to determine whether complex geometries significantly impede the inspection and to develop body-inspection strategies.

FY 2008 Accomplishments

- The team completed the evaluation of the first generation array and probe holder on three BIW structures. The BIW evaluations involved constructing inspection plans, inspecting over 100 beads with a wide variety of geometries and probe orientations, and generating evaluation reports. Over 80% of the adhesive structure could be imaged at a speed of over 1 m/min with this feasibility system. These images elucidate large scale features such as adhesive spread and the fill-factor of the flange. The 1 mm resolution also allows small features such as surface springback, air entrainment, bead dribbles, and weld expulsion damage to be imaged.
- The project team designed, built, and evaluated a second generation ultrasonic array and probe holder that is intended as a production prototype. This device is simpler and smaller than the first generation and should be able to inspect 95% of the BIW while imaging 85% of the area under the probe. The system works with a commercially available closed-loop water circulation system and should have a significantly reduced system cost
- A new signal processing effort was initiated to reliably extract the adhesive thickness from the ultrasonic array echo data. This analysis can rapidly compensate for probe to surface distance variations.
- The ability of ultrasonic inspection to accurately predict the bond strength was tested. On flat coupons, nondestructive measurements of the bond area and the bond thickness can predict the strength to within 10% over 90% of the adhesive bead. The primary shortcoming is that the scaling law presently underpredicts the bond strength at the beginning of the adhesive bead. This is the area where the peel crack is initiated.
- Reproducible procedures for constructing weak (kissing) bond samples using a wide variety of contaminants and controlled cures were established. Multiple sets (nine) of samples were produced with reduced shear strength. The strength ranges are from 10% to 100%. Two types of contaminants were added throughout the bond strength range. Over 150 strength tests were completed to characterize the weak bonds. NDI evaluations using ultrasonic and other NDI methods are underway. The resulting images could be correlated to the subsequent strength measurements. Some initial promising results have been obtained from several methods but additional study is necessary before any conclusions can be made. This will be the focus of the activities in the last year of the project.

Future Direction

- In the final year of the project, the second generation ultrasonic array system will be deployed on BIW samples at Sandia National Laboratories and one U.S. Council for Automotive Research (USCAR) facility. This development effort is geared to improve inspectability and reliability, reduce overall system cost, and to reach a production-ready system. This will include a written procedure for probe deployment on automotive flanges,
 - Ultrasonic signal analysis to determine reliably the bead thickness and quality of all adhesive/adherent interfaces will be pursued as funding allows.
 - The final year will also complete the study of inspection methods to detect weak bonds. The technologies selected primarily include advanced ultrasonic technologies.
 - Funding for fiscal year (FY) 2009 is an issue. The continuing resolution within the federal government will only allow quarterly step funding. Deliverables and timing have been modified to accommodate the budget.
-

Introduction

Adhesive bonding is an important joining tool for modern automotive structures. Structural adhesives can greatly increase the strength as well as stiffness of joints and can significantly improve the crash performance of vehicles. Structural adhesives also allow more efficient structures to be designed that may be difficult to weld. Structural adhesives will play an increasingly important role in the joining of dissimilar materials such as aluminum (Al) to steel or magnesium (Mg) to other metals: the adhesive acts both as a galvanic barrier and as a stress spreader on materials that are more brittle.

The NDE601 project is directed at filling a major technical gap for adhesives: how to determine whether an adhesive bond on a vehicle will perform as designed without actually destroying the bond, that is, how to nondestructively inspect the adhesive and assure that the bond has its designed strength. This year we completed verification of the wedge peel method as a new, high spatial resolution method that can quantify the variation of bond strength along long bond lines and with the presence of contaminants. In this period it was shown that ultrasonic measurements can accurately predict wedge peel strengths.

The major goal of the previous phase of this project was to select and develop an NDE method to inspect automotive flange joints when the adhesion was good. After evaluating several alternatives, ultrasonic pulse/echo inspection with a manually scanned linear array was targeted as a

near term solution. A unique phased array probe system with a closed-loop circulation system was built by the team and successfully passed testing on over 150 flat coupons. Over 100 m of adhesive bonding were imaged.

This year the evaluation of this first generation ultrasonic array system was completed. In this round, the entire adhesive bonds on three production car bodies were subjected to inspection. This allowed issues of inspection plan organization, report generation, accessibility, ultrasonic coupling, operator skill, and operator ergonomics to be evaluated. The system performed quite well delivering high resolution images of the adhesive area, perhaps the most important element of needed inspection.

Based on the performance of the Gen 1 probe, a second ultrasonic probe system was designed specifically for automotive adhesive bond inspections. This is targeted as a production-intent system. This custom array and probe were built, assembled, and tested and shown to significantly improve accessibility and reduce system cost.

Extensive work was also completed on bonds that have intimate contacts but are weak: so called kissing bonds. Several new contaminants, in addition to grease, were shown to reproducibly reduce bond strength. It was shown that grease reduces both shear and tensile strength with the same sensitivity dependence and that grease contamination can be detected with ultrasonic pulse/echo inspection. A large suite of coupons

with reduced bond strengths were built for a round robin test of advanced inspection methods.

Mechanical Strength Characterization of Automotive Adhesive Joints

Ultimately, the selected NDI methods need to predict the failure loads of adhesively bonded joints. This project has both evaluated load measurement methods and tested bonds with varying bond width, thickness, and contamination. From this earlier work, a wedge-peel destructive test was selected as the method of choice. This method can handle wide variations in bond strength over short distances and can handle spot welds that are used along with adhesives (weld bonding).

The wedge-peel method uses an instrumented load frame to pull a standard wedge (ISO11343) through the adhesive bond as seen in Figure 1. The load vs. displacement curve can be compared with either an NDE image obtained before peeling such as ultrasonic through transmission or with the actual peel surface (see Figures 2 and 3 for examples). The ultrasonic through transmission has been our gold standard since it tests all the interfaces and the time-of-flight gives the location bond thickness.



Figure 1. Wedge peel fixture at USCAR

Simple adhesive strength laws based on bond width and thickness are adequate for predicting the wedge peel strength if the bond strength varies over multicentimeter length scales. Figure 2 shows a prediction of bond strength for a sample with

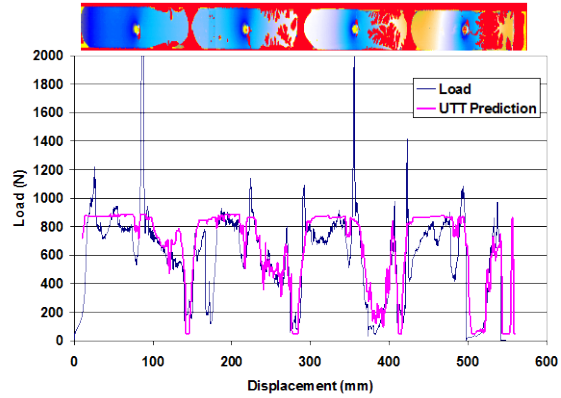


Figure 2. Adhesive wedge-peel strength compared with scaling law prediction based on UT-TT measurement of bond width and thickness (see image insert below).

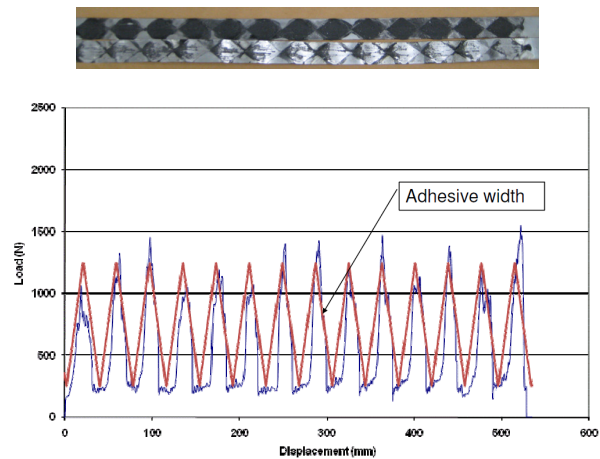


Figure 3. Adhesive wedge-peel strength for the diamond shaped bond pattern shown in the image insert. This demonstrates the effect of varying crack length when the failure load varies rapidly.

severe springback and large adhesive thickness variations.

The predicted strength is typically within 10% of measured over 90% of the bead length. The major errors occur at the spot welds and at the leading edge of the bond where the crack is initiated.

To test the limits of simple strength laws, additional samples with more rapid strength variation were made such as the diamond shaped adhesive bond in Figure 3. This shows more significant departures from the simple scaling law predictions. This is understood to arise from the crack length which varies throughout the test. This

moves the crack tip back and forth relative to the displacement location. These conditions will require a dynamical prediction of strength rather than a scaling law.

In previous work, it was shown that the bond shear strength of these automotive adhesives could be systematically reduced by a precisely applied grease layer. Oil- and grease-tolerance is a feature of automotive-grade adhesives that are required/designed to work directly on surfaces that are coated with mill oil. This year, the wedge-peel strengths of similar greasy bonds were measured. It was found that both the wedge peel strength (mostly Type 1 failure) and shear strength (mostly Type 2 failure) had the same relative dependence on the amount of grease contamination.

Ultrasonic Pulse/echo Technologies

After extensive testing in the first year of the project, ultrasonic pulse/echo using linear ultrasonic arrays was selected as the target inspection technology when there is good bonding. Linear array probes are comprised of many small piezoelectric elements, each of which are individually wired and can be controlled independently. A focused, ultrasonic beam is generated and electronically scanned along the array axis transverse to the bead and manually scanned along the bead. At each location, a short ultrasonic pulse is launched through the outer adherent and the train of echoes from the various adhesive-adherent interfaces is detected; variations of interface reflectivity and echo delay times are used to determine the joint condition.

While ultrasonic pulse/echo technologies have been available for many decades, only recently have they become portable and practical tools. Besides the earlier cost and complexity, the primary barriers for using this on the automotive plant floor have been the complex joint geometries and the thinness of the sheets (0.7 to 3 mm) that dictate high frequency transducers and cause difficulty in analyzing the ultrasonic echoes.

This year saw major milestones reached on the path towards implementing linear ultrasonic arrays as a production inspection technology. The evaluation of the Gen 1 ultrasonic phased array

probe on three production car bodies was successfully completed. A second generation scanner, designed specifically for automotive flange inspections, was built and tested. Limited progress on signal processing was made. In addition, four different pulse/echo inspections have been applied to weak (kissing) bonds samples.

Deployment of the Gen 1 Linear Array Probe on Production Bodies

The four goals of the BIW assessment were: (1) create inspection plans for each BIW, i.e., record deployment information for each adhesive bead such as metal stackup, location, bead length, and probe orientation, (2) develop a manual scanning procedure that optimizes the beam coupling to the surface and maximizes the inspection area, (3) construct a matrix of features and rate the system performance, and (4) document the bead images along with images of the BIW.

Currently the system is configured in a C-scan mode using simple time gating in order to inspect the first adherent/adhesive interface. This provides a rapid, high resolution scan of the adhesive bead position and area. The system can scan at up to 1 meter per minute with 1mm resolution. This is more than enough to inspect 100 meters of adhesive in an off-line, two hour inspection window.

These inspections included two premium sedan BIW bodies with extensive adhesive bonding (20–30 m per vehicle) and a truck floor subsystem with embedded discrepancies. Over one hundred individual bead areas were imaged over the three bodies. Two examples are shown in Figure 4. This figure shows the rear passenger floor pan of a car along with the blue/white C-scan images of adhesive wet-out area. The variation of the bond width along the flange is readily seen, including the spread around each spot weld. Closer examination of the images show features such as surface springback, air entrainment, bead dribbles, and weld expulsion damage.



Figure 4. Floor section of the A-body showing the phased array scans positioned next to the imaged area.

Several flange configurations are present on the OEM BIWs including hem flanges. The specimens include mild steel bonded to Al and mild steel with several production adhesives. All adhesives are in an uncured state. The three bodies gave a good inventory of different flange designs currently in production and different flange orientations. Vertical flanges presented no special difficulties.

An inspection procedure was also developed that explains the operation and maintenance of the equipment.

Gen 2 Linear Array Ultrasonic Scanner

Based on the Gen 1 experience, a second linear array system (Gen 2) was designed and built. Figures 5 through 9 show the Gen 2 prototype probe and the water delivery system. This system is less than half as wide as the Gen 1 while having comparable inspection width and the same 1 mm resolution.

The linear array can be seen at the middle of the probe holder in Figure 5. This shows how the probe holder width has shrunk to the probe length; the blind area between the array and the probe holder envelope is dramatically reduced. The new probe is half as tall and 30% shorter than the Gen 1 probe. Figure 6 shows the probe being

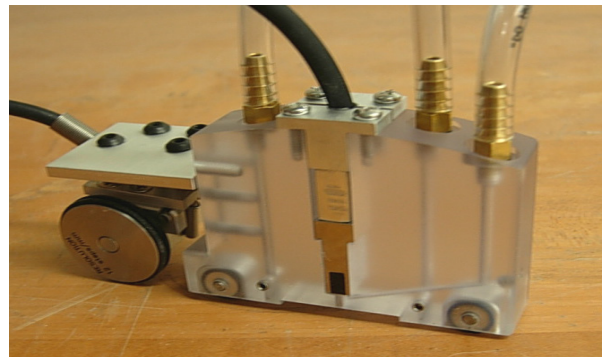


Figure 5. High frequency linear array embedded in a custom probe holder (Gen 2).

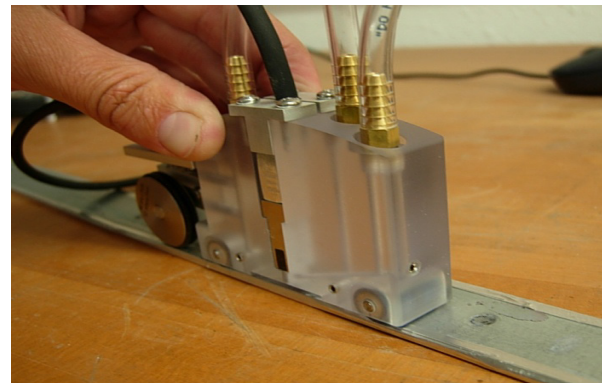


Figure 6. Linear array probe holder and encoder on a wide weld-bonded coupon.

scanned along a flat coupon that is similar to an automotive flange that is weld bonded.

This configuration of the probe uses a wheel encoder to measure the location of the probe along the bead. The encoder is spring mounted to more accurately follow the flange curvature. The encoder can also be raised so that the probe can be placed in narrow U-channels. In another configuration, the wheel encoder is removed and a string encoder is used.

The miniaturization of the probe (technical advance) will also allow flanges with smaller radii of curvature to be inspected. Figures 7 and 8 show BIW flanges being inspected.

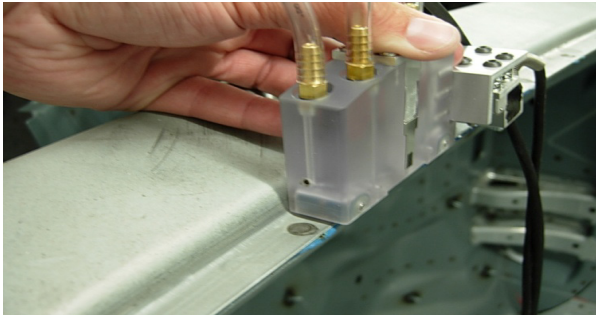


Figure 7. Linear array probe holder and encoder on BIW flange. Note: the probe now rests on a curved flange.

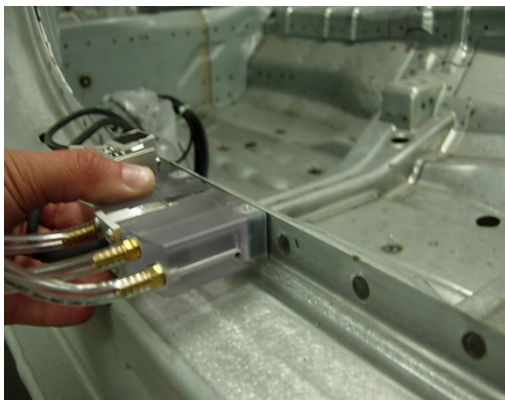


Figure 8. Linear array probe holder and encoder on BIW flange (side position).

The holder uses a closed-loop water circulation system to maintain a water column between the array and the flange surface. One angled inlet port supplies the water to the array while the two vertical ports vacuum excess water from the part (Figure 5 far right port is the water supply). The redesigned water column system is much simpler and allows a commercially available, closed loop

water system to now be used (see Figure 9). It includes a filtered water supply, return pump, simple valve, and water aspirator. This water delivery system is in a self contained shipping case.



Figure 9. The closed-looped circulation system is commercially available.

The Gen 2 system performance was validated on flat test specimens. Again the system is configured in a C-scan mode using simple time gating to inspect the first adherence-adhesive interface. This system can scan at up to 5 meters per minute with 1 mm resolution. Ultrasonic images comparing performance from the Generation 1 and 2 probes are shown in Figure 10. The test sample selected was 1.5 mm aluminum weld bonded to 1.5 mm aluminum. The contrast, signal to noise, and sensitivity uniformity of the two array systems are comparable. The phased array resolution is comparable to an ultrasonic inspection using an immersion tank, i.e., about 1 mm.

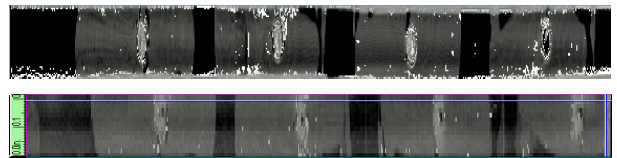


Figure 10. Ultrasonic image comparison between Generation 1 (top image) and Generation 2 (bottom image).

The next step will be to exercise the Gen 2 system on the large BIW samples especially on areas that were not inspectable by the Gen 1 system.

Preliminary Pulse/echo Signal Analysis

The short burst of high frequency sound waves travels through the material with some loss of energy and is reflected at any interface. The reflected echo signal is captured and analyzed to determine the presence and location of reflected interfaces. Variations in reflectivity or scattering can be used as the basis of flaw detection. Transit times of the echoes can be used to assess bond-line thickness.

Dr. Steve Neal, University of Missouri—Columbia, was placed under contract with Sandia National Laboratories. Dr. Neal has extensive knowledge in ultrasonic signal analysis and post processing techniques. His work in the area of correlation coefficients for ultrasonic detection has potential as a post processing technique for adhesive thickness measurements. This method was able to compensate for variations in the water column height over the sample scan in approximately 1 sec at PC analysis speeds.

Simulations of the echo train were used to evaluate different analysis strategies. These echo simulations were accurate for up to six reflections in the top sheet even for thin adherents (0.8 mm thick) with closely spaced echoes. However, Dr. Neal concluded that the reduced amplitude echoes from the adhesive-second sheet interface are too small to be extracted on stackups with sub-millimeter sheets and typical adhesive thicknesses with the current arrays and array controller. Dr. Neal's report is stored in the USCAR project archives.

Work on determining the limits of analysis on stackups with thicker sheets will be pursued depending on project funding.

Weak (Kissing) Bond Samples

A procedure to make weak bond samples reproducibly was developed at USCAR. This procedure has been transferred to Sandia National Laboratories for further development. This stage of work is devoted to testing the performance of advanced NDI methods that are reported to be sensitive to weak bonds, and to quantifying their ability to correlate with the reduced bond strength. This includes looking for small-scale variations in

the bonded interface. The data analysis will look at subtle changes in the response and signal trends in order to link differences to bond quality parameters.

The adhesive manufacturing matrix of test coupons included three structural adhesives identified by the USCAR representatives. The test coupons were designed to be larger than the USCAR production flanges. The increased area is necessary to properly assess all advanced NDI methods. Six similar coupons were fabricated for each variable identified by USCAR. Three of these samples were pulled to assure the sample set bond strength and three will be used for NDI inspection assessments. Figure 11 displays the test coupon drawing and material specifications.

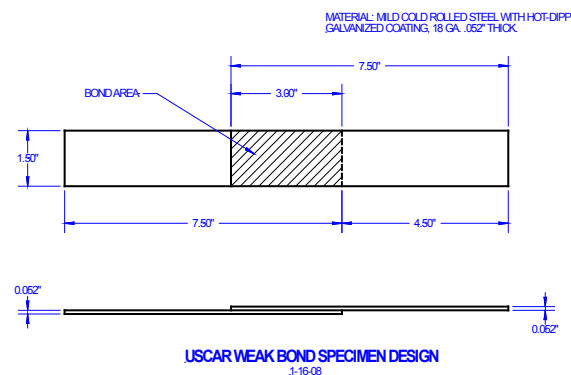


Figure 11. Test coupon for weak bond assessment. The contaminate is added to the bond line adhesive before curing takes place.

Conclusions

Steady progress was made on the project objectives during the second full year of funding. The first generation linear ultrasonic array tool for off-line inspections was successfully tested on production vehicles. While this ultrasonic array system is currently only able to inspect the wet-out on the outer skin, the system performance appears to be adequate to allow the adhesive mapping. The second generation version of this ultrasonic array scanner is now being built and is the final prototype development. It improves the performance on narrow flanges and on curved surfaces. The high resolution wedge-peel test has been established as a bond strength standard. Simple scaling laws allow NDI measurements of bond width and thickness to predict the bond

strength over a wide range of conditions. Finally, promising results were obtained from the USCAR transferred technology to Sandia National Laboratories to produce weak-bond samples.

Acknowledgements

This project team consisted of members from the automobile industries, federal research laboratories, and universities. The team members were: Ciji Nelson, Kirk Rackow, Steve Neil, Kim Lazarz, Dan Ondrus, Dave Biernat, Jessica Schroeder, John Fickes, Ray Bis, Mike Golden, Dave White, Rajat Agarwal, Bill Brown, Kent Wen and Marvin Klein. We also would like to thank IOS and Olympus NDT for their input and Mittal Steel and Novellis for supplying metal blanks.

References

1. *NDE601-FY2006 Annual Progress Report for DOE ALM*, Joseph DiMambro and Dennis P. Roach, Sandia National Laboratories and Cameron J. Dasch, General Motors Research & Development, December 15, 2006.
2. *Engineering Report on NDI of Adhesively Bonded Mild Steel Flat Coupons for USCAR/USAMP Project NDE 601—NDI of Adhesive Metal Bonds*, Cameron Dasch, Joe DiMambro, John Fickes, Jessica Schroeder, Jim Lazarz, Dan Ondrus, Dave Biernat, Raj Agarwal, Ray Bis, and Andy Terry, February 15, 2008.
3. *Draft Engineering Report on NDI of Adhesively Bonded Flat, Aluminum Coupons for USCAR /USAMP Project NDE 601—NDI of Adhesive Metal Bonds*, Cameron Dasch, Joe DiMambro, Ciji Nelson, John Fickes, Jessica Schroeder, Kim Lazarz, Dan Ondrus, Dave Biernat, Raj Agarwal, Ray Bis, Andy Terry, and Dave Sigler, August 14, 2008.
4. *NDE601-FY2007 Annual Progress Report for DOE ALM*, David G. Moore and Joseph DiMambro, Sandia National Laboratories; and Cameron J. Dasch, General Motors Research & Development, December 12, 2007.
5. *NDE601-FY2008 Mid-year Progress Report for DOE ALM*, David G. Moore and Ciji L. Nelson, Sandia National Laboratories; and Cameron J. Dasch, General Motors Research & Development, May 15, 2008.
6. *Final Report Phase 1: Developing Ultrasonic Signal Analysis Tools for Metal/Metal Adhesive Bonded Joints*, Steven Neal, September 15, 2008.

Presentation/Publications/Patents

1. Disclosure of Technical Advance Dated February 20, 2007, “*Probe Deployment Device for Optimal Ultrasonic Wave Transmission and Area Scan Inspections*,” Joseph DiMambro, Dennis Roach, Kirk Rackow, and Ciji Nelson, Sandia National Laboratories, and Cameron Dasch, General Motor Corporation.
2. *Correlating Adhesive Bond Strength with Non-Destructive Test Methods*, K. Lazarz, C. Dasch, and R. Agarwal, presented at the Annual Meeting of the Adhesion Society, Austin TX, February 2008.
3. *Nondestructive Inspection of Adhesive Bonds in Automotive Metal/Metal Joints (NDE 601)*, C. J. Dasch, USAMP Off-site Review, October 29, 2008.
4. *Using Quantitative Ultrasonic NDE to Accurately Predict Adhesive Bond Strengths*, Cameron Dasch, Kim Lazarz, and Rajat Agarwal, Quantitative Nondestructive Evaluation Conference, Chicago, IL, July 2008.

B. Laser Ultrasonic Inspection of Adhesive Bonds Used in Automotive Body Assembly

Principal Investigator: Marvin Klein

Intelligent Optical Systems

2520 West 237th Street

Torrance, CA 90505

(424) 263-6361; fax: (310) 530-7417; e-mail: mklein@intopsys.com

Technology Area Development Manager: Joseph A. Carpenter

(202) 586-1022; fax: (202) 586-1600; e-mail: joseph.carpenter@ee.doe.gov

Contractor: Intelligent Optical Systems

Contract No.: DE-FG02-06ER84545

Objective

- Adhesive bonding is widely used in automotive production, especially for body assembly. It is critical to be able to measure the strength of adhesive bonds during manufacture in a nondestructive, effective and rapid manner. There are no current means for inspecting these bonds in real time. The specific inspection requirement is to: (1) map the adhesive spread, (2) measure the thickness over the full area, and (3) measure the bond strength. All inspections must be performed from one side and must be able to function on contoured surfaces with ~1 mm resolution. The ideal tool must be able to perform the above measurements simultaneously (i.e., in one pass across the bond). In this project we have applied the technique of laser ultrasonics to the adhesive-inspection requirements described above. The specific goals of this project are to determine the best inspection configuration and signal-processing approach, followed by the development and demonstration of a prototype inspection system.

Approach

- The technology which we will apply to this inspection requirement is laser ultrasonics, in which a pulsed laser beam is directed to the surface to generate ultrasonic waves in the sample, and a continuous-wave laser receiver is used to detect the waves after they interrogate the required sub-surface feature and return to the surface. Laser-based ultrasonic inspection has a number of benefits over transducer-based ultrasonic inspection, including: (1) lack of physical contact with the workpiece; (2) high spatial resolution obtained using focused laser beams; (3) high scan rate associated with rapid beam scanning; and (4) high bandwidth, thereby improving the measurement accuracy.
- This project is closely coordinated with Sandia National Laboratories' phased-array project, "Nondestructive Inspection of Adhesive Metal/Metal Bonds," funded by the Department of Energy (DOE). The United States Council for Automotive Research (USCAR) Nondestructive Evaluation (NDE) Working Group acts as an advisory group. The fore mentioned project has produced a large number of adhesive-bonded specimens. The flat specimens vary in adhesive, adherent type and thickness, stackup (2–3 layers), cure state, and surface contaminants. These conditions bound the processing parameters for the adhesive assembly process. These specimens have been used to optimize the beam configuration and signal-processing techniques. The remaining portion of our project is devoted to the development and demonstration of a prototype scanning inspection system that can be scaled to a measurement speed of 1 meter/minute.

Accomplishments

- In 2008, we completed months 4–15 of a 24-month Small Business Innovation Research (SBIR) Phase II project that started in 2007. During the course of this effort, we tested a number of steel and aluminum specimens prepared for the Sandia project, thus improving our ability to determine the configuration of both

laser beams (separation, size, shape, energy) that provides the best signal-to-noise. We have identified an algorithm for processing the raw signals to provide accurate mapping of the adhesive spread. Finally, we have engineered a measurement head that is based on the required beam configuration and that is intended to be integrated into a robot-based prototype inspection system.

Future Directions

- In 2009 we will complete the software and hardware development required for assembly and testing of the prototype inspection system. This system will be demonstrated for interested parties.

Introduction

Adhesive bonding is widely used in automotive production, especially for body assembly. The most common use is the lap joining of two or three sheet-metal panels. Adhesive bonding adds strength, and thus allows the use of lighter components at equal performance. Adhesive bonding allows the joining of dissimilar materials such as aluminum (Al) and steel. Modern adhesives (especially epoxy resins) have excellent fatigue and thermal shock resistance, and less critical design tolerances because of their gap-filling capabilities. Their service range extends from space environments to high temperatures. It is critical to be able to measure the strength of these bonds during manufacture in a nondestructive, effective, and rapid manner.

The most important manufacturing issues that can influence the strength of an adhesive bond are the maintenance of the proper fit-up and proper surface preparation. While adhesive bonds are tolerant of some range of gap between the panels, if the gap is too large, the adhesive will not cover the required area, and the intrinsic strength of the adhesive itself is reduced. If surface contamination (e.g., oil, grease, surface oxides, corrosion, and water infiltration) is present, the bond adhesion will be reduced. In the limit of very low adhesion, weak bonds may have intimate contact, but little or no bond strength (“kissing”).

The corresponding requirements for nondestructive evaluation of adhesive bonds fall into three areas: (1) mapping of the adhesive coverage, (2) measurement of adhesive thickness, and (3) measurement of the adhesion of each metal/adhesive bond.

All inspections must be performed from one side and must be able to function on contoured surfaces. The ideal tool must be able to perform the above measurements simultaneously (i.e., in one pass across the bond).

At the current time, nondestructive inspection is not performed during the bonding process. The only quality control techniques now implemented are careful process control, machine-vision inspection of the adhesive bead before joining, and selective destructive evaluation. A nondestructive technique for in-line measurement of adhesive integrity would reduce scrap and warranty costs, and thus allow wider use of adhesive joining.

Laser ultrasonics offer an attractive approach for nondestructive evaluation over a broad range of applications. The full complement of ultrasonic waves (longitudinal, shear, Lamb, and Rayleigh) can be produced with known directionality. The pulses are high in bandwidth, thereby providing the high depth resolution required for thin sheets and bonds. The spot sizes on the part can be much less than 1 mm in diameter, thereby providing high spatial resolution.

The objective of this project is to develop a real-time system for inspection of adhesive panels during auto body assembly (see Figure 1). This system will incorporate a fiber-delivered robotic measurement head containing a scanning mirror that will be able to scan narrow sections of adhesive very rapidly.

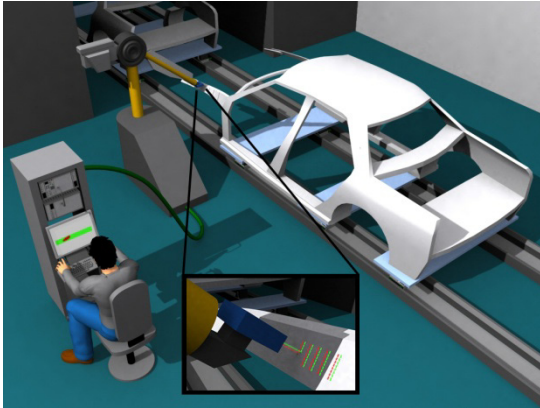


Figure 1. Depiction of robot-driven inspection system performing a two-dimensional scan of an adhesive-bonded auto body panel.

Samples Provided

General Motors and the project carried out at Sandia National Laboratory were kind enough to provide a number of samples for testing in 2007. The samples consisted of a two sheet stackup with three adhesive joints distributed along the length of the samples, each joint having a spot weld near the center. A number of plate thicknesses and adhesives were included among the samples. In 2007, we were able to obtain clear scans of these samples in the through transmission configuration that provided mapping and thickness measurement with good accuracy.

In 2008, we continued to use these samples for the continued development of the pulse echo configuration, and for software development. We also received samples with varying bond strength from Sandia that were prepared for their project. There were 10 samples with bond strength that varied from 11% to 88%. The goal in this case was to develop a measurement technique and algorithm that could measure the bond strength.

Samples Scans

A typical map or C-scans of a portion of Sample A3 obtained in through-transmission is shown in Figure 2. This amplitude map clearly captures the adhesive spatial coverage with sharp edge definition, limited only by the 1 mm step size.

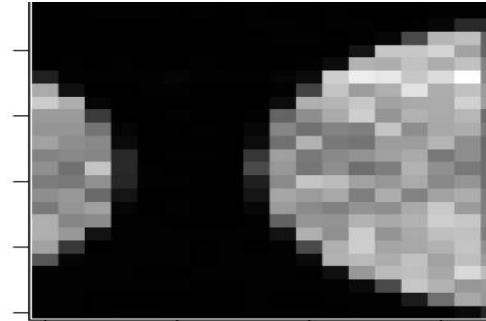


Figure 2. Through transmission zoom image of a portion of Sample A3. Step size = 1 mm.

All subsequent measurements were performed with both beams on the same side (pitch-catch configuration) and spaced 1–2 mm apart. In this configuration, multiple echoes are expected from both the A and B interfaces (with A being the adhesive interface closest to the measurement head, and B being the adhesive interface furthest away from the measurement head). The value of the reflectivity at these interfaces is dependent on the impedance values of each material. Specifically, the reflectivity of a steel/adhesive interface (~0.9 in amplitude) is smaller than that of a steel/air interface (very close to 1.0). This difference is not large, but it is sufficient to yield a measurable difference in the amplitude of the reflected waves from the A-interface.

In pulse-echo we obtained C-scans by windowing on a late-arriving echo in order to take advantage of multiple reflections from the A interface and thus amplify the expected amplitude difference. A typical pulse echo C-scan of a portion of sample A3 is shown in Figure 3.

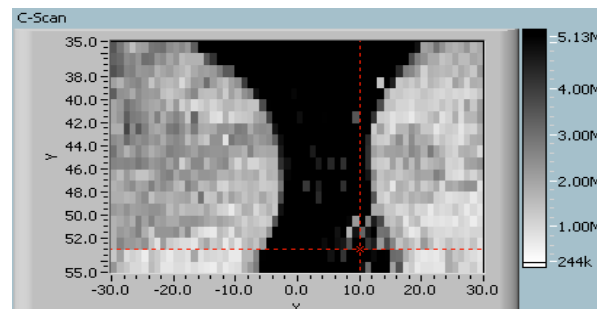


Figure 3. Pulse echo zoom image of a portion of Sample A3. Step size = 1 mm.

We have also obtained data on aluminum Sample K26. Typical A-, B- and C-scans are shown in Figures 4 to 6. In the A-scan, the back wall echoes in a region without adhesive are strong. The cursors shown in this figure identify the time gate used for the C-scan of Figure 6.

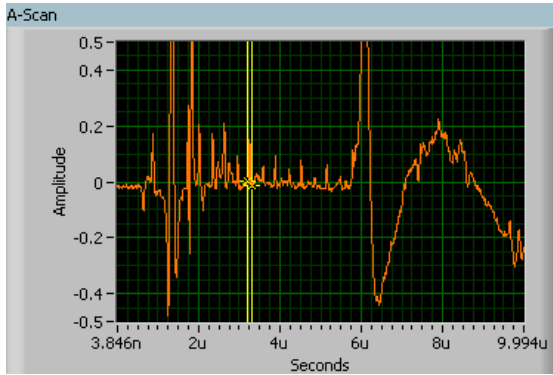


Figure 4. Typical A-scan on Sample K26.

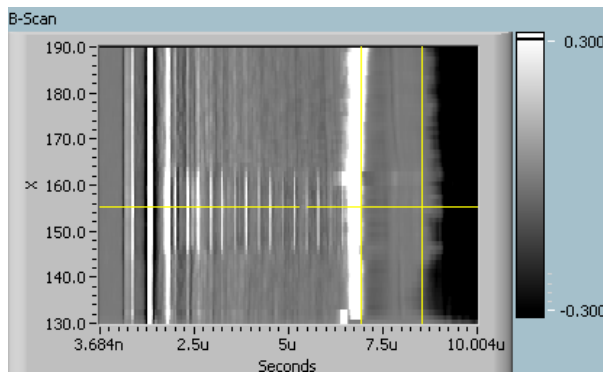


Figure 5. Typical B-scan on Sample K26.

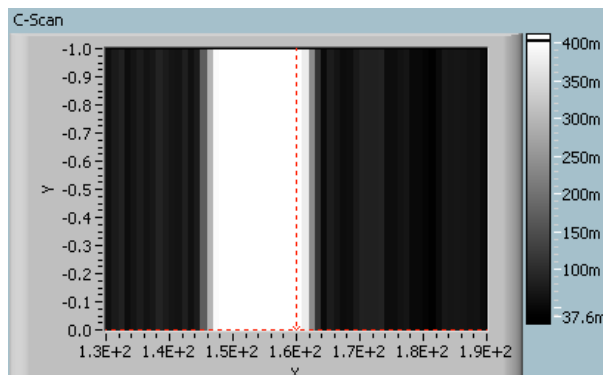


Figure 6. Typical 1D C-scan on Sample K26, based on the amplitude in the window defined in Figure 4.

The B-scan shows the dramatic difference in signals between the adhesive at low values and high values of X, and the gap near X =

150–160. It is clear that the aluminum and adhesive are nearly impedance matched, so the A-interface echoes are very weak. The C-scan of Figure 6 was taken in only one direction, and is based on the amplitude of the signal in the cursor-defined window shown in Figure 4. Note the large contrast that results from the strong differences in the signals shown in the B-scan of Figure 5.

Signal Processing Development

We have made good progress in mapping the adhesive spread. In order to map the adhesive thickness, it is important to clearly identify and measure the echoes from within the adhesive. We are developing an approach that involves enhancing of the B-scan features using line-finding techniques applied to the images.

The line-finding approach is illustrated in Figure 7. The raw B-scan image is processed by a MATLAB based algorithm that identifies lines and tracks them.

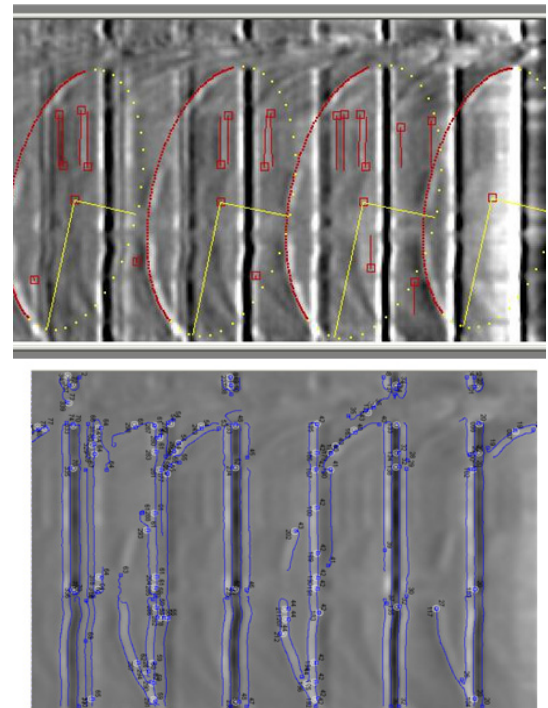


Figure 7. Line-finding technique applied to two adhesive B-scans taken on the same sample.

The straight lines represent echoes in the top sheet and the curved lines represent echoes in the adhesive. Both are easily identified. Once the echoes are identified, a separate algorithm can find arrival time of the adhesive echoes in order to determine the adhesive thickness.

Measurement Head Development

As a result of the testing we performed, we have redesigned and simplified the measurement head. In the prior design, the generation beam consisted of five separate beams derived from a single pulsed laser and delivered through a fiber bundle. Our testing determined that the beam separation and delivery system was subject to optical damage. In the new design, an off-the-shelf pulsed laser with a fiber pigtail is being used, with a single 1 mm core fiber delivering the generation beam to the measurement head. The detection and signal beams are now routed from a single optical module that is self-aligning. The new head is much simpler and less prone to optical damage than the previous one.

Conclusions

In 2008, good progress was made on the overall project objectives.

We have successfully applied laser ultrasonics to the requirement for evaluating adhesive bonds used in auto body assembly. Techniques have been developed to map the adhesive spread and measure the thickness. The signal processing efforts have indicated a pathway for processing the raw data in real time. We have designed prototype scanning hardware that will be robot-mounted for automated measurements. Continued work in 2009 will be required to refine the signal processing and complete the development of a prototype.

Presentations/Publications/Patents

1. Marvin Klein and Homayoon Ansari, "Laser Ultrasonic Inspection of Adhesives Used in Auto Body Manufacture," *First International Conference on Laser Ultrasonics*, Montreal, Canada, July 16–18, 2008.
2. Marvin Klein and Homayoon Ansari, "Laser Ultrasonic Inspection of Adhesives Used in Auto Body Manufacture," *ASNT Topical Conference on Automotive Industry Advancements with NDT*, Greenville, SC, May 11–12, 2009.

C. Online Nondestructive Weld Quality Monitor and Control with Infrared Thermography

Principal Investigator: Zhili Feng

Oak Ridge National Laboratory

P.O. Box 2008, Oak Ridge, TN 37831-6095

(865) 576-3797; fax: (865) 574-4928; e-mail: fengz@ornl.gov

Principal Investigator: Hsin Wang

Oak Ridge National Laboratory

P.O. Box 2008, Oak Ridge, TN 37831-6064

(865) 576-5074; fax: (865) 574-3940; e-mail: wangh2@ornl.gov

Technology Area Development Manager: Joseph A. Carpenter

(202) 586-1022; fax: (202) 586-1600; e-mail: joseph.carpenter@ee.doe.gov

Field Technical Monitor: C. David Warren

(865) 574-9693; fax: (865) 574-6098; e-mail: warrencd@ornl.gov

Contractor: Oak Ridge National Laboratory (ORNL)

Contract No.: DE-AC05-00OR22725

Objective

- Develop an infrared- (IR-) thermography-based weld-quality detection technology capable of reliable and cost-effective online nondestructive monitoring and feedback control of welding assembly operations in high volume auto production environment.
 - Phase I: Demonstrate the technical merit and potential of the IR-based weld-quality monitoring technology for resistance spot welds (RSWs).
 - Phase II: Conduct a field demonstration of a prototype system for real-time welding operation monitoring and online weld-quality evaluation, including technology transfer and dissemination for future commercialization.

Approach

- Produce welds with different levels of quality and geometry attributes.
- Catalog and quantify weld-quality attributes by means of destructive characterization.
- Develop quantitative correlation between various weld-quality attributes and their characteristic IR thermal signature through combined welding heat-flow simulation and laboratory IR experiments.
- Develop field-deployable IR measurement techniques for cost-effective detection of the characteristic thermal-signature patterns during welding operations (real-time) and/or in online postmortem inspections.
- Develop efficient IR data analysis algorithms for thermal-signature recognition.
- Integrate the field-deployable IR measurement system and the data analysis algorithm to develop a prototype IR weld-quality monitor and control expert system for field demonstration.

Accomplishments

- Identified and ranked weld-quality attributes in RSWs for IR-based inspection through industry survey.
- Produced and characterized an initial set of controlled RSWs with various types and levels of quality attributes.
- Completed a comparative study on various heating and cooling approaches for IR-thermography measurement for postmortem online inspection.
- Performed initial computer simulation of heat-flow pattern in RSWs with varying weld-quality attributes to identify most effective experiment set-up for IR measurement.

Future Direction

- Phase I:
 - Complete the evaluation and “down-select” the heating/cooling method for postmortem IR thermography.
 - Complete feasibility evaluation of real-time IR thermography.
 - Complete computational simulation and establish the theoretical basis for IR-inspection sensitivity.
- Phase II:
 - Determine the sensitivity of IR signals obtained in real time to the weld-quality and production environment.
 - Develop the IR thermal-signature recognition algorithms of the expert system for postmortem inspection.
 - Expand to wide range of weld and materials combinations.

Introduction

Welding is an essential technology used in auto-body structure assembly. Variations in welding conditions, materials, part dimensions, and other production conditions inevitably occur in the high-volume and highly complex auto-body assembling process, resulting in variations of weld quality and “out-of-tolerance” situations which impair the quality and performance of the vehicles. Despite extensive research and development (R&D) efforts over the years, nondestructive weld-quality inspection remains a critical need in the auto industry, largely due to the unique technological and economical constraints of the auto production environment—any weld-quality inspection technique must be fast, cost-effective, low in false rejection rate, and nonintrusive (i.e., not interfere with the highly automated welding fabrication process).

The goal of this project is the development of a prototype, field-deployable, online weld-quality monitoring system based on state-of-the-art IR thermography. IR thermography detects surface temperature changes due to geometric discontinuity or inhomogeneity. A distinct advantage of IR thermography as a nondestructive

evaluation (NDE) tool is its nonintrusive and noncontact nature, making it especially attractive in high-volume production environments. IR for weld-quality inspection in the auto-assembly environment has been explored in the past, mostly postmortem. The development so far has been unsuitable for implementation in the mass-production environment of the auto industry.

Working with industrial partners, we recently demonstrated several novel concepts and approaches that would overcome some of the key technical barriers inhibiting the use of IR thermography as an effective weld NDE tool in auto assembly lines. A unique advantage of the ORNL approach is the potential for real-time weld-quality detection as the weld is being produced. This would offer the opportunity of real-time welding process feedback for in-process adjustment and control.

This project builds upon our recent work, and consists of a two-phase, gated R&D effort to further advance the IR-thermography-based weld-quality monitoring and control technology to a stage that can be deployed in high-volume auto production environments. The first phase is a 12-month Concept Feasibility study. Started in

May 2008, Phase I focuses on further improving ORNL's IR thermography approach, establishing the scientific basis, and demonstrating the ability to detect various types of defects (lack of bonding, cold weld, porosity) and determining the critical weld-quality attributes (weld size and indentation) in RSWs produced under the welding practices used by the industry.

At the end of first phase (Gate 1), decisions will be made with respect to the technical merit, the effectiveness, and the potentials of the IR-based weld-quality monitoring and control methodology. If warranted, more comprehensive R&D will be performed in the second phase (Technical Feasibility) study, leading toward eventual field demonstration of the technology. The second phase will also include identifying and partnering with potential technology transfer and commercialization entities.

The R&D in Phase I has been primarily carried out at ORNL, with support from the industry collaborators. An industry technical advisory committee has been formed for this project, consisting of representatives from Chrysler, Ford, General Motors, and ArcelorMittal.

Based on the recommendations of the industry advisory committee, Phase I includes exploratory studies on both real-time and postmortem IR thermography to determine the feasibility of the two different approaches for weld-quality inspection. The real-time approach detects the weld quality as a weld is being made by detecting the changes in temperature patterns during welding, whereas the postmortem approach applies an external heat source after a weld is made such that the inspection is performed as a separate step after welding. Both approaches can be implemented for online inspection. According to the industry advisory committee, the two different approaches address different application needs.

From May to September 2008, Phase I focused on the following tasks:

- producing the initial set of controlled RSWs with various types and levels of weld-quality and defect attributes,

- comparatively studying various heating and cooling approaches for IR-thermography measurement, and
- producing the initial computer simulations of heat-flow patterns during IR-thermography measurement.

RSW Samples for IR Thermography

An initial set of RSW samples has been produced for use in the postmortem IR-thermography study. This set of samples was designed to cover the range of weld defects and quality attributes that are commonly encountered by the industry and are known to influence the structural performance of the spot welds in auto-body structures. These attributes are listed below, in the order of decreasing importance according to the industry advisory committee:

- weld with no or minimal fusion,
- cold or stuck weld,
- weld nugget size,
- weld expulsion/indentation,
- weld porosity, and
- weld cracks.

To ensure consistency in producing different levels of weld defects and quality attributes, all welds were made at the welding laboratory of ArcelorMittal's R&D center, according to the specifications of the project. ArcelorMittal, a primary steel supplier to the automotive industry, has extensive experience in welding procedure development and qualification for applications of advanced high-strength steels in automotive body structures.

All welds were made on hot-dipped galvanized DP 590 steel of 1.85 mm nominal thickness, in the common two-stack configuration. For each welding condition, a total of six replicate welds were made. Two of the six replicates were sectioned destructively to determine the weld nugget size and type and degree of weld defects. The other four welds of the same set were used in IR-thermography measurements. In addition, extensive IR measurements were also conducted on one of the sectioned welds before it was sectioned.

Representative weld cross sections are provided in Figure 1 through Figure 5.

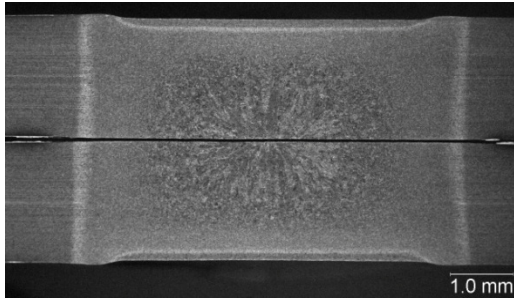


Figure 1. Cross-sectional view of a stuck weld with very small fused weld nugget.

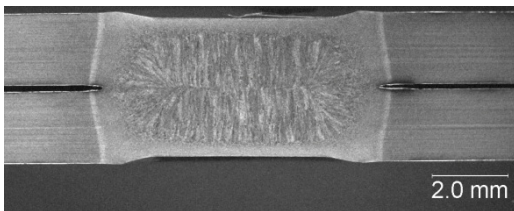


Figure 2. Cross-sectional view of a weld with acceptable weld nugget size and no defect.

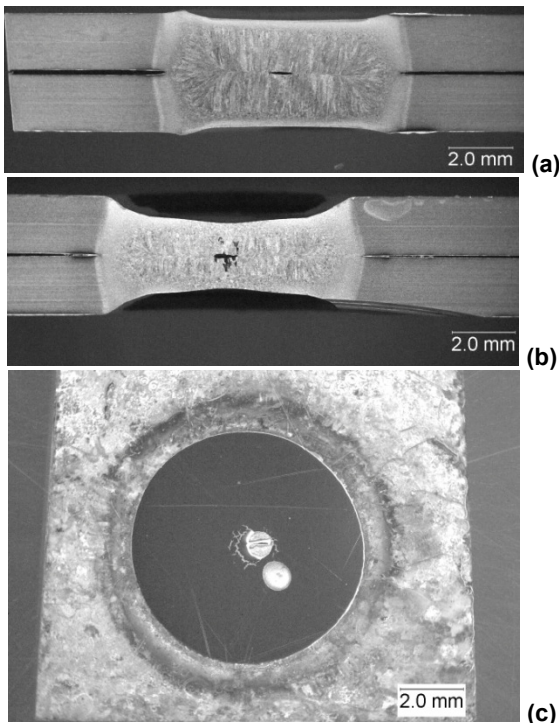


Figure 3. Welds with solidification shrinkage voids as revealed in cross-sectional view, (a) and (b), and by machining off one of the steel sheets (c).

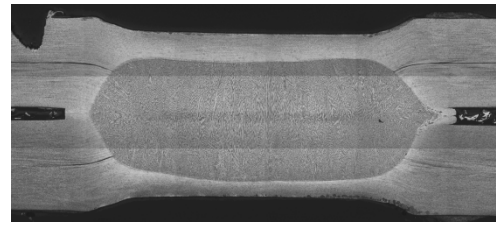


Figure 4. Cross-sectional view of a weld with expulsion.

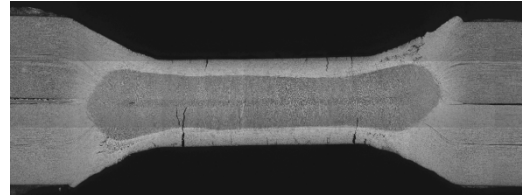


Figure 5. Cross-sectional view of a weld with expulsion, cracking, and surface indentation.

Table 1 summarizes the welds made for different weld defects and quality attributes. Each set of welds is characterized by its weld nugget size, surface indentation, and type and/or extent of defects. The weld nugget represents the fused region of the weld, and its diameter was determined under optical microscope from both the cross-section samples and the samples with one of the sheet steels carefully removed by machining and polishing to the faying surface of the weld.

Table 1. Weld samples with different weld-quality attributes for postmortem IR measurement.

Condition	Weld IDs	Weld Nugget (mm)	Void Dia (mm)	Indent (mm)	Est. Brassing	Cracking
Stuck Weld	34-39	0	None	0.06	None	None
Undersized weld	53-58	4.15	None	0.17	None	None
Minimum weld	65-70	5.8	None	0.21	None	None
Maximum weld	99-104	6.3	None	0.24	None	None
Void A	93-98	6.2	0.7	0.32	None	None
Void B	87-92	6.3	1.4	0.27	None	None
Indent/crack	117-122	7.4	None	0.62	None	None
Indent/crack	124-129	6.6	None	1.84	None	None
Indent/crack	131-136	6.6	None	1.04	Light	Yes
Indent/crack	138-143	7.9	None	1.72	heavy	Yes

Evaluation of Heating/Cooling Methods for Postmortem Inspection

In postmortem IR inspection, an external heating source is applied to induce transient temperature changes in the weld and its surrounding area. For the same effect, a cooling source can also be used. An IR-thermography camera is strategically placed near the weld to detect the characteristic temperature changes and relate the changes of weld quality. The measurement principle is illustrated in Figure 6. The type of the external heating or cooling sources and the way they are applied will influence the heat flow in the weld and thereby the sensitivity and accuracy of weld defect and quality attribute detection.

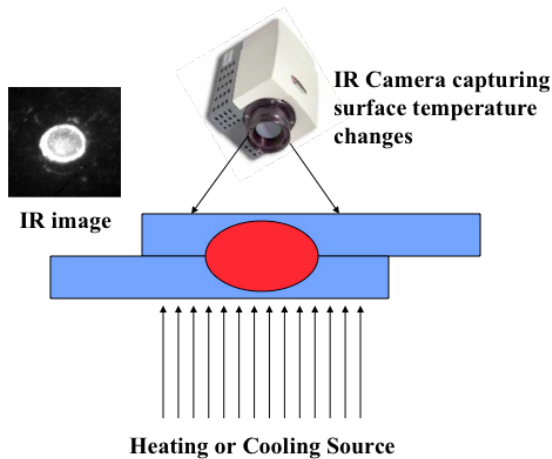


Figure 6. IR weld-quality inspection principle (postmortem approach).

In this task, different heating and cooling methods were evaluated for their suitability for postmortem IR inspection. The method of choice should be capable of generating a noticeable temperature change (10 to 20°C) and subject to easy and quick manipulation of the duration of heating or cooling (from subsecond to several seconds). Factors related to suitability in the auto-body assembly environment such as cost, reliability, and automation must also be considered in selecting the heating/cooling method.

Several methods were evaluated in this task. They included two heating methods (a xenon flash lamp and a hot-air gun) and three cooling methods (ice cubes, a cold-air gun, and a commercial gas duster).

Xenon Flash Lamp. The flash lamp had adjustable controls for the heating duration and power, resulting in relatively consistent tests among samples. With a high power and duration of around 8 milliseconds (ms), the flash was treated as a pulse function.

Ice Cubes. Ice cubes had unique advantages over most of the other methods. Because ice is always at a constant 0°C when melting, the temperature at the contact point can always be assumed to be consistent. Also, since the ice melts on contact, the liquid layer creates a very conductive area through which heat can be transferred, resulting in the surface temperature condition of 0°C during the test. However, the presence of liquid water during the test and the physical contact between the cooling media (ice tube) with the workpiece are two major drawbacks of this technique.

Cold-Air Gun. A Vortex Tube, which is a device that causes compressed air to separate into hot and cold regions, was used to generate the cold air. Hot air is expelled through a radiator, while cold air is blown out a nozzle. The air from the nozzle was approximately 8°C but could be varied slightly by varying the pressure of the compressed air used.

Hot-Air Gun. An industrial strength hot-air gun, similar to a personal hair dryer only capable of much higher temperatures, was used to generate the hot air. The heat gun did not allow for precise temperature control; however, it was capable of producing the largest temperature difference of all the methods tested, around 200°C.

Gas Duster. The final cooling method tested was a gas duster (Figure 7). Most commercial gas dusters are filled with a volatile liquid such as difluoroethane, which has a boiling point of -25°C. When turned upside down, the canister nozzle releases the chemical in liquid form, which quickly evaporates at room temperature. This method exhibited the advantage of greatest controllable temperature difference created, allowing for relatively large distinctions between spot welds.

It is a common practice in IR thermography to treat the measurement surface with chemicals or



Figure 7. Commercial gas duster. When used upright, gas is expelled through the nozzle to clean dust from keyboards and electronics. When turned upside down, liquid difloroethane is expelled.

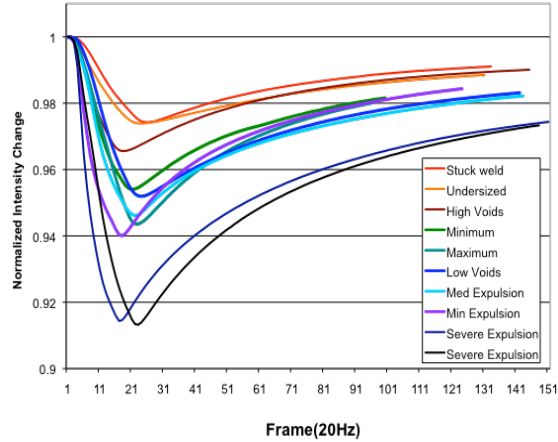


Figure 8. Intensity curves of controlled welds with different weld-quality attributes generated using the gas duster cooling method.

paints to provide better contrast or clarity for the IR images. Because such treatments or coatings of spot-weld surfaces are prohibited on automotive production lines due to the cost and production rate concerns, surface treatments were purposely avoided in our experiment. Instead, the IR images were digitally enhanced during image analysis.

Temperature change was measured using an IR camera with a capturing rate at either 60 Hz or 20 Hz, depending on the length of time and method used. Using the series of images and computer software, the change in IR image signal intensity measured over time was plotted and compared for welds with different quality attributes. Examples of the characteristic heating/cooling curves obtained by different heating/cooling methods are given in Figure 8 and Figure 9. In these figures, the IR signal intensity was normalized with respect to the baseline IR intensity before applying the external heating/cooling source to the weld region. The normalization made it possible to differentiate the thermal-signature patterns associated with different levels of weld defects and quality.

Figure 8 compares the surface temperature changes (as represented by the intensity of IR measurement) of different welds using the gas duster as the cooling medium. It is evident that

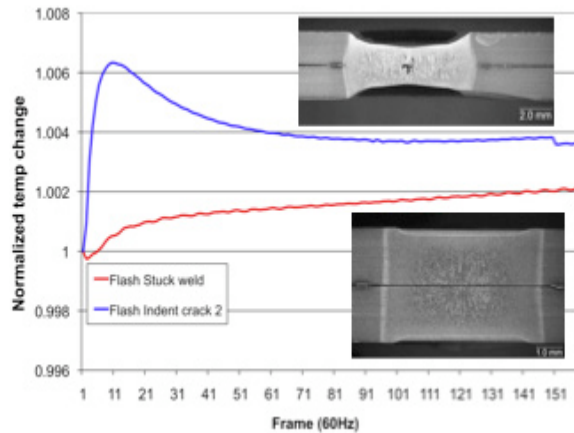


Figure 9. Intensity curves of a stuck weld and a cracked weld with heavy indentation as measured with xenon flash lamp heating method.

welds with different defects and geometry attributes have distinguishable temperature transient profiles. More encouragingly, the transient temperature curves can be roughly grouped into three distinct groups corresponding to the weld quality: (1) the welds with the acceptable quality are in the middle pack of the curves; (2) the welds with unacceptable quality attributes such as stuck welds, undersized weld (weld diameter less than the minimum specification by the industry), and high volume of voids or porosities are shown in the upper pack of the curves; and (3) the welds with severe expulsion and cracking are distinctively in the lower pack of the curves.

Figure 9 shows the normalized intensity curves measured by means of the xenon flash lamp heating method for two different types of defects: stuck weld vs weld with severe surface indentation due to expulsion. The thermal responses are clearly different for the two different cases.

In addition, the IR measurement results appeared to be highly consistent. This is illustrated in Figure 10 using the ice cube cooling method. Two different types of welds with known quality problems, stuck weld or weld with severe surface indentations, were tested. For each weld condition, five replicate welds were used. It is evident from these results that the IR thermography technique is highly repeatable and consistent.

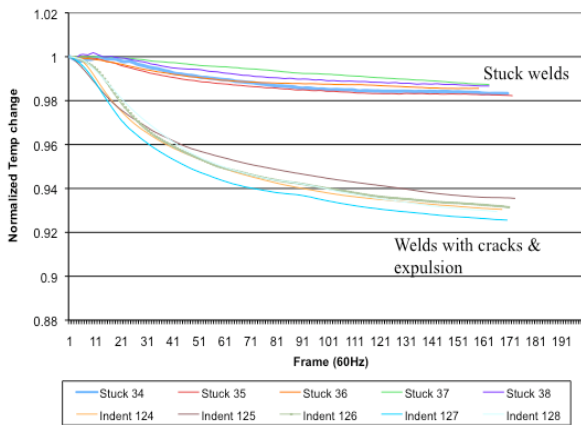


Figure 10. IR measurement on replicate welds using the ice cube cooling method.

The above findings clearly suggested the feasibility of IR thermography for weld-quality inspection.

Computational Simulation

Initial computer simulations of the heat flow by postmortem external heating were carried out as part of the Phase I work.

The purposes of the simulations were (1) to establish the analytical basis for quantitative correlation of various weld attributes with the heat-flow and temperature patterns caused by the external heating/cooling source, and (2) to provide information on the optimal heating/cooling arrangement and IR thermal-image data collection and analysis to maximize the resolution and

sensitivity of defect detection and to minimize the inspection time necessary for eventual assembly-line implementation.

The finite-element heat-flow simulation matrix included a series of weld nugget sizes, surface-indentation depths, sheet thicknesses, voids, and cracks to represent the weld-quality attributes. It also included various heating patterns, heating times, and heating-intensity levels.

Figure 11 shows the simulation results for three representative cases: a cold weld with minimal fusion bonding (Case1), a normal weld (Case 2), and a weld with excessive indentation and

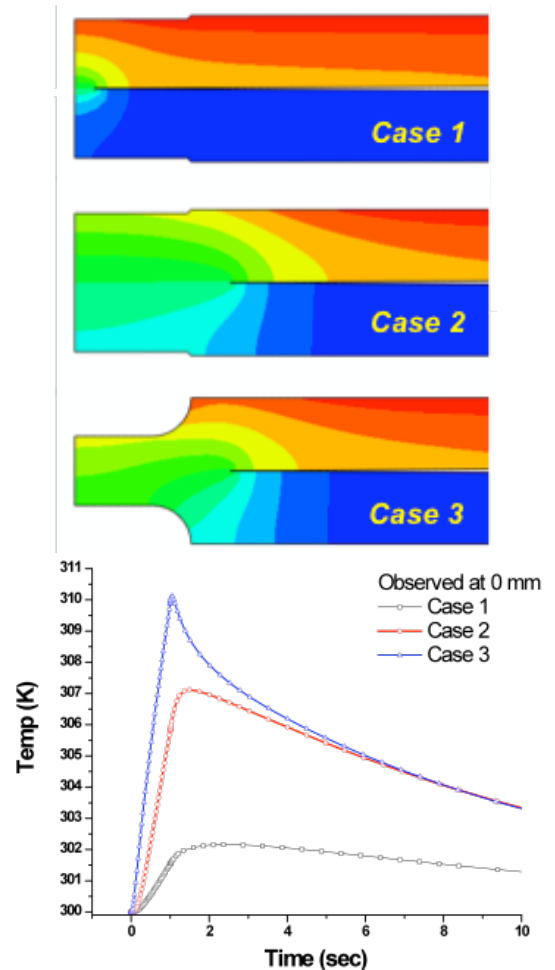


Figure 11. Thermal signatures of three representative welds of different quality obtained from heat-flow simulation.

expulsion (Case 3). The simulation clearly shows that there are intrinsic thermal signatures (heating

rate, cooling rate, peak temperature, etc.) associated with welds of different qualities. These characteristic thermal signatures are the scientific basis for IR-based weld-quality detection technology. The computational simulation results are being analyzed and used to develop the IR thermal-signal-recognition expert system for weld-quality detection.

It is interesting to compare the temperature variation with time in Figure 11 and Figure 8. The observed grouping of cooling curves by weld quality in Figure 8 is clearly supported by the simulation of the intrinsic heat-flow characteristics of welds with different qualities in Figure 11.

Conclusions

The initial study conducted in fiscal year 2008 suggested the potential of IR thermography as a spot-weld quality-inspection technique. Welds having different quality attributes exhibited distinctive temperature transients that were readily measurable by IR thermography. Finite-element heat-flow simulation revealed that the observed distinctive temperature transients were indeed related to the differences in weld qualities.

Presentations/Publications/Patents

1. W. Woo et al., "Application of Infrared Imaging for Quality Inspection in Resistance Spot Welds," SPIE Defense, Security and Sensing Conference, Orlando, Florida, April 13–17, 2009.

D. Enhanced Resonance Inspection for Light Metal Castings (NDE701*)

Principal Investigator: Xin Sun

Pacific Northwest National Laboratory

P.O. Box 999, Richland, WA 99352

(509) 372-6489; fax: (509) 372-6099; e-mail: xin.sun@pnl.gov

Principal Investigator: Martin H. Jones

Nondestructive Evaluation Laboratory, Ford Motor Company

(313) 805-9184; fax: (734) 458-0495; e-mail: mjone147@ford.com

Technology Area Development Manager: Joseph A. Carpenter

(202) 586-1022; fax: (202) 586-1600; e-mail: joseph.carpenter@ee.doe.gov

Field Technical Monitor: Mark T. Smith

(509) 375-4478; fax: (509) 375-4448; e-mail: mark.smith@pnl.gov

Contractor: United States Automotive Materials Partnership (USAMP) and Pacific Northwest National Laboratory (PNNL)

Contract No.: DE-FC26-02OR22910 and DE-AC06-76RL01830, respectively

Objective

- To ensure the structural integrity of light metal castings by satisfying the need for rapid, reliable nondestructive evaluation (NDE).
- To assess the capability of modeling approaches to predict accurately the vibrational mode and variability of frequencies.
- To evaluate quantitatively the sensitivity of resonance inspection (RI) to anomalies of various types and sizes in various locations.

Approach

- Manufacturing acceptance of RI is limited by its empirical methodology; therefore, augment current empirical methodology with predictive tools. Initially use a “simple” part and compare experimental and finite-element analysis (FEA) predictions of resonance frequencies and shapes.
- Develop a set of tools to enable predictive capability:
 - Make current setup/training time shorter by using computer modeling to simulate response of actual parts and flaws.
 - Identify response to critical flaws thereby allowing “fault” to be specified and subsequently fixed (process feedback).
- Model to translate materials properties and geometry into predicted frequencies:
 - Use computer-aided design (CAD) model or preferably three-dimensional (3D) scanning to provide exact as-is geometry to FEA model.
 - Generate FEA 3D mesh directly from scanned data.

*Denotes Project 701 of the Nondestructive Evaluation Working Group of the United States Automotive Materials Partnership, one of the formal consortia of the United States Council for Automotive Research set up by Chrysler, Ford, and General Motors to conduct joint, precompetitive research and development (see www.uscar.org).

- Methods to identify mode shapes for each frequency:
 - The ability to identify exact modal shapes is critical in determining what frequency changes correspond to which features in the part.
 - Will need to perform for all modes in practical sampling range of approximately 1–80 kiloHertz (kHz).
- Sensitivity matrix for critical anomalies:
 - From FEA only, predict the response sensitivity to a specified feature (flaw) anywhere in the part.
- Validate by comparing predicted and measured frequencies and mode shapes:
 - Have multiple vendors collect data over full frequency range and compare these experimental results with FEA predictions.
- Complete approach by performing same steps for a more “complicated” real-world part.

Accomplishments

- Connecting rod testing completed:
 - Automatic identification of modes based on comparison of calculation and laser vibrometer measurements.
 - Dimensional check of CAD model using computed tomography (CT)—discrepancies found.
 - Accurate prediction of mode frequencies.
- Calculations based on both CAD model and CT data:
 - Extensive numerical testing of efficient variational method to predict resonance shifts for porosity and slits (oxide film model).
- Real-world part (automotive knuckle casting) testing and modeling completed:
 - In-plant selection of parts.
 - Resonance measurements of the parts by Quasar, The Modal Shop (in-plant), and Polytec.
 - Precision material property measurements (1 part in 10,000).
 - 3D dimensional measurements (1 part in 1000) by computed tomography.
 - Finite-element natural frequency extraction of knuckle and mesh sensitivity study.
 - Modal analysis and steady state dynamic analysis for knuckle casting.
 - Correlation of predicted mode shapes between measured resonance peaks.

Future Direction

- Work on frequency shift prediction for connecting rod and knuckle parts.
- Prediction of flaw size and location based on RI spectral data to be tested.

Introduction

The ability to use RI for testing and flaw identification has been long desired. The RI technique is quick and sensitive, making it an ideal choice in production environments. This project set out to determine if it is feasible to make RI more usable in everyday testing. There are several ways this might be accomplished: decrease the required size of the training set, choose the frequencies to watch more intelligently, predict the sensitivity of the test to a specific feature, and the like. Because of the complexity of the resonance structure in even simple parts, computer modeling

of the RI process has been deemed intractable in many instances.

This project has shown that modeling the resonant behavior of simple parts is not only possible but also quite accurate. Simulated and experimental results from three commercial vendors (The Modal Shop [TMS], Magnaflux Quasar, and Polytec) were compared. It was shown that the use of laser vibrometry resolves ambiguities as to the actual mode shape present at a particular frequency.

During this project, there has been great progress in casting real-world parts, experimental testing,

and cooperation with and between commercial partners. Progress has been made in automating mode identification and in predicting accurate mode frequencies. Additionally, errors were identified in the CAD model of the connecting rod part through the use of CT inspection, and 3D computer-aided engineering (CAE) meshes of the part directly from the CT scan data were generated.

Frequency calculations have been performed with CAD and CT data. A computationally efficient variational method to predict resonance shifts for porosity slits (oxide film model) and slots (more crack-like model) have been implemented, and the results are encouraging.

The project demonstrated that finite element and variational principle-based computational methods can be used to model and predict accurately the natural frequencies and vibrational mode shapes of a real-world part. A more realistic part with complex surface features yields better correlations between predictions and measurements because of shorter wave length (i.e., higher frequency) needed to trigger any possible mode switches between the predicted and measured frequency spectra.

Approach

Automatic Identification of Modes Based on Comparison of Calculation and Laser Vibrometer Measurements

The project identified the need to provide the exact resonance mode occurring at any given frequency, which is necessary to compare experimental and CAE results. A commercial partner specializing in laser vibrometry, Polytec, measured the actual motion of the parts as they were being acoustically excited. A practical problem was quickly obvious: many of the resonance modes are similar in frequency and shape.

PNNL went through the early results and correlated the measured mode shapes from Polytec data with the finite element-predicted modes by carefully looking at each mode by hand (eye) and making the assignment. Aside from being tedious, this process is difficult to do under the best of

conditions. A method of performing comparison by evaluating a surface integral over the part was proposed and implemented by PNNL as a computer program. The results were examined by several skilled individuals and found to be accurate. Figure 1 gives a comparison of the hand performance with the computed correlation.

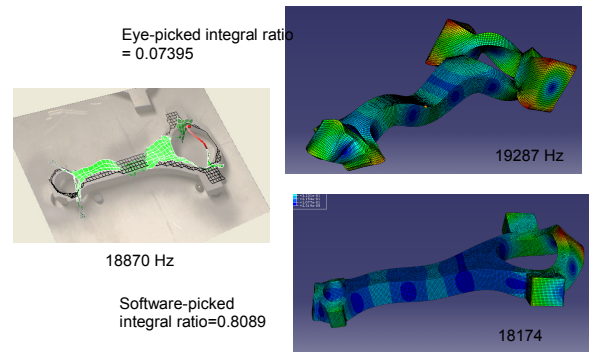


Figure 1. Mode shape comparison.

Because this technique relies on an analysis of the actual/predicted physical movement of the part, it is impervious to computational errors. In fact, it correctly identifies the mode shapes even in the presence of errant model data and predicted frequencies, as discussed in the next section. This has become the final arbiter in the identification of experimental and calculated mode shapes.

Dimensional Check of CAD Model Using Computed Tomography (CT)

The connecting rod was originally designed in CAD as a 3D solid part, and necessary drawings were also generated from the CAD system. Early predictions of the resonant frequencies based on the CAD model were not as accurate as hoped (Figure 2). When the CT-based model of the data became available, it was discovered that it was showing a thickness of 18.00 millimeters (mm), whereas the actual part measured 19.75 mm. It was also found that the diameter of the holes in both ends were undersized in the CAD model by ~1.0 mm each.

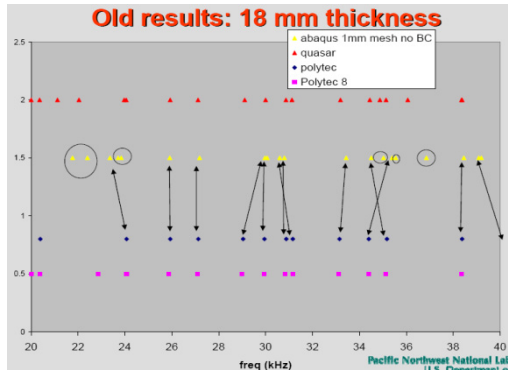


Figure 2. Comparison between predictions and various measurements based on original CAD dimensions. Note: shifts in frequency (angle of arrows) and switches (crossing arrows) became available.

Upon investigation, it was found that the parts were cut from material plate already on hand in the machine shop, hence the change in thickness. Water-jet cutting of the shapes also allowed the diameter to grow slightly with the depth of the cut: the “top” of the holes is slightly smaller in diameter than the “bottom.” Predictions made with models containing the correct thickness based on the CT data yielded more accurate results and made correlation and analysis more satisfying all around (Figures 3–5).

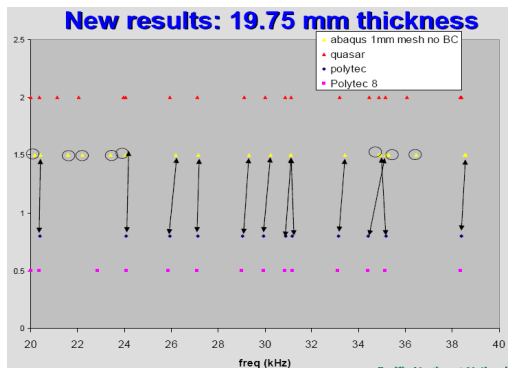


Figure 3. Comparison between predictions and various measurements 20-40 kHz based on as-built dimensions.

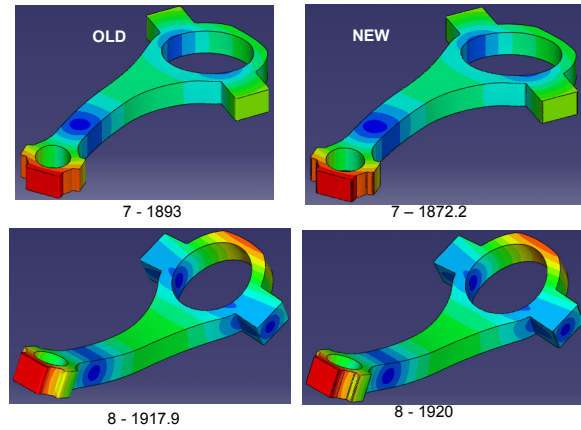


Figure 4. Comparison of old and new model sizes on resonant modes: low frequencies.

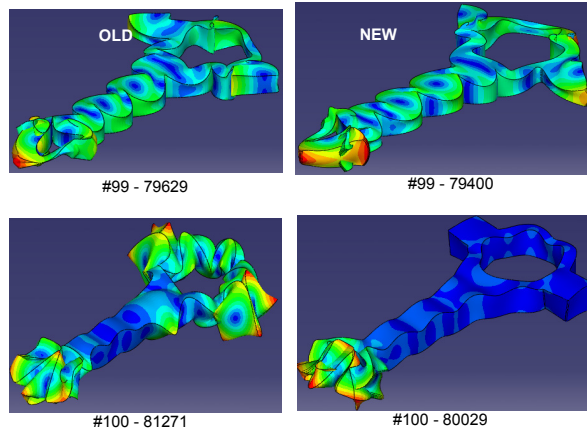


Figure 5. Comparison of old and new model sizes on resonant modes: high frequencies.

Accurate Prediction of Mode Frequencies

Calculations based on both CAD model and CT data have been carried out and analyzed. The CAD model has been corrected for the observed errors and the results predicted from CAD- and CT-based data are essentially the same. Figure 6 shows the full spectrum of predicted, experimental RI and laser vibrometry (Polytec) measured data. The predicted frequencies are quite close and within the expected error due to geometry, material properties and measurement error.

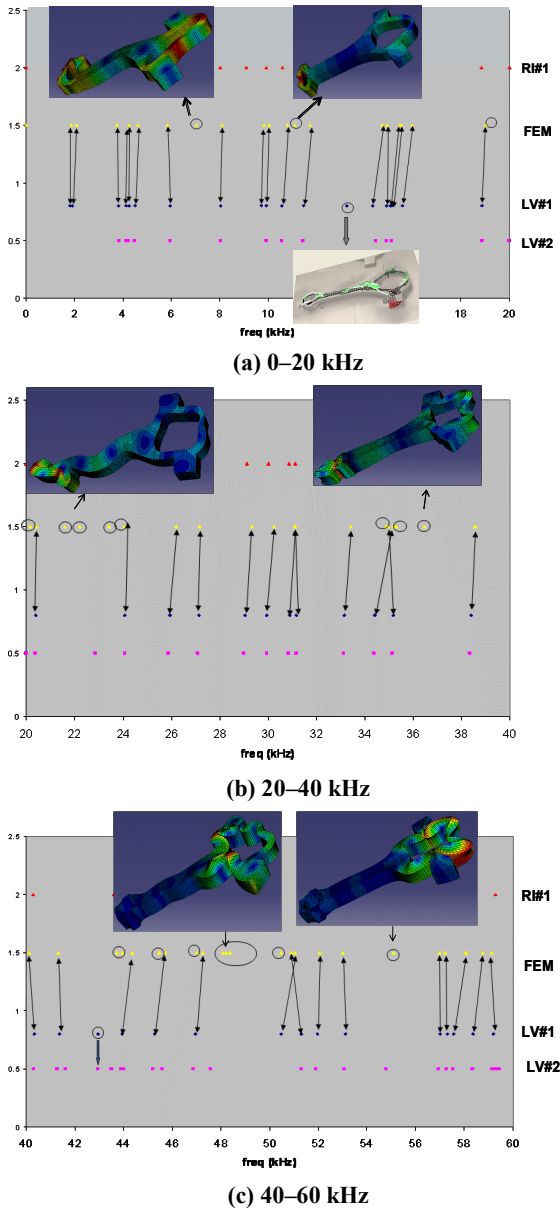


Figure 6(a)–(c). Comparison of predicted and measured frequencies.

Implementation of Computationally-efficient Variational Method to Predict Resonance Shifts for Porosity and Slits (Oxide Film Model)

The effect of different types of flaws (features) on the resonant frequencies has been tested extensively. There are examples of porosity (missing material in a small internal region) slits, where surfaces are free to move but with no gap when at rest (Figure 7) and slots where a small straight line of mass has been removed as a way to simulate a small crack’s behavior (Figure 8).

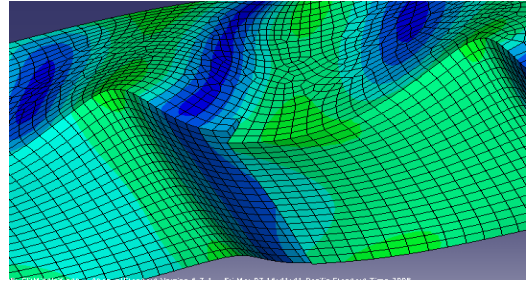


Figure 7. A slit in motion due to RI excitation. Note the surfaces are free to move but have no gap when at rest.

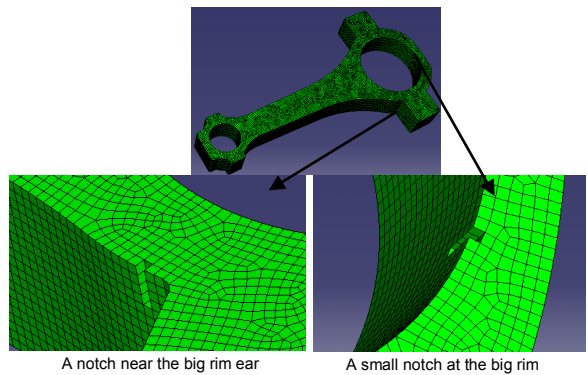


Figure 8. An example of a slot.

When analyzed, these features suggest that for small features, the frequency shifts obey superposition laws (i.e., the effects of each feature can be evaluated independently and summed with all other shift forces at the end; Figure 9).

<ul style="list-style-type: none"> ▶ Goal: detectability of multiple defects ▶ Can linear superposition be used to predict frequency shift when there is more than one defect in the part?
<ul style="list-style-type: none"> • A notch in a part produces a frequency shift Δf_1 for every mode • Second notch produces a frequency shift Δf_2 for every mode • If both notches are small, so Δf_1 and Δf_2 are both small, will the frequency shift be $\Delta f_1 + \Delta f_2$ with both notches?
<p>▶ Result from Abaqus simulation validates this assumption</p> $\Delta f_{1+2} \approx \Delta f_1 + \Delta f_2$

Figure 9. Rational for frequency shift linear superposition.

Linear superposition makes computing the frequency shift from a given feature easier to calculate and allows computation of the sensitivity to an RI test to any feature. The sensitivity calculation continues to be the subject of

refinement but is good and usable at this time (Figure 10).

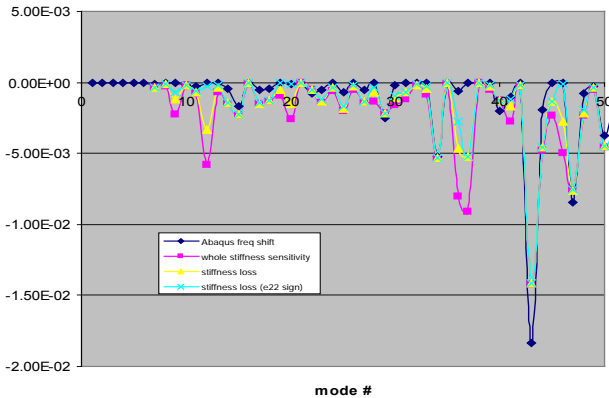


Figure 10. ABAQUS prediction vs stiffness sensitivity.

Real-world Part with Complex Surface Features—Knuckle Casting

With the selection of an automotive knuckle casting (Figure 11) as the target part, an event was held at the casting supplier’s facility. A population of 150 parts was selected based on X-ray and dye penetrant inspection. Quasar and TMS tested all 150 parts in the plant and recorded the full spectrum resonance measurements of each.



Figure 11. An automotive knuckle chosen for testing.

Figure 12 shows the detailed spectra comparison between Quasar and TMS in the frequency range of 30–40 kHz. Overall good agreement has been achieved, with several frequency peaks called out by Quasar but not by TMS, possibly due to the low energy input delivered at high frequency levels by the hammer impact used by TMS.

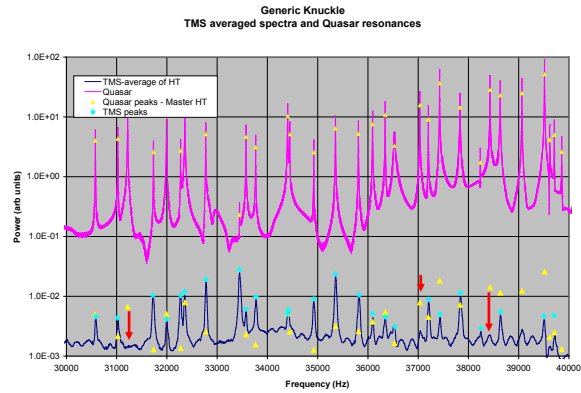


Figure 12. Frequency spectra measured for the knuckle by Quasar and TMS with extracted peaks.

The actual part geometry obtained from the CT scan was used to generate the finite element model (FEM) using Shrinkwrap of Hypermesh (Figure 13). The finest mesh that can be generated using Hypermesh Shrinkwrap is 0.8 mm, below which the finer details of the surface finish of the knuckle require extensive surface repair prior to meshing. The material properties for the finite element analysis are obtained using resonance spectroscopy with small cuboids machined from the knuckle at various locations. The isotropic material model fits the measurement data with high accuracy: density = 2.6711 g/cm³, Poisson’s ratio = 0.3358, Young’s modulus = 73.8989GPa.

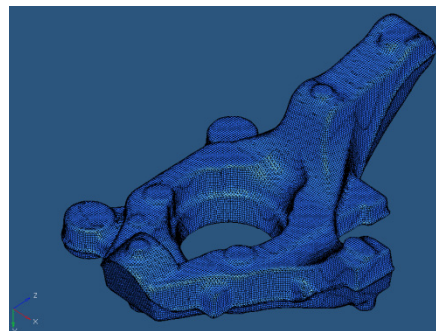
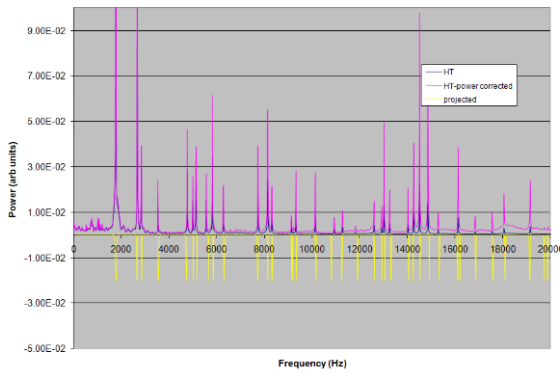
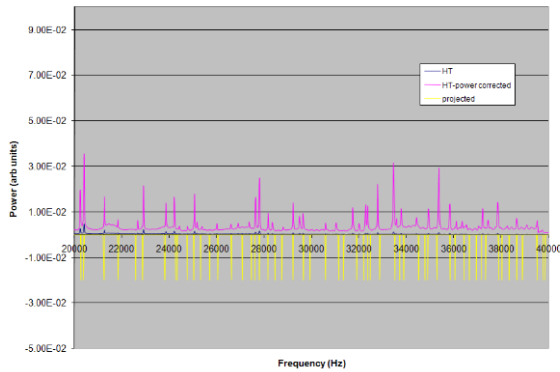


Figure 13. Typical finite element mesh used for the knuckle with 1.75 mm mesh size.

Mesh size convergence study was carried out from 2 to 1.2 mm. The finite-element-predicted frequencies for the knuckle presented in Figure 14 are 99.65% of the frequency values calculated with 1.2 mm mesh, based on the mesh size convergence study.



(a) 0-20kHz



(b) 20-40kHz

Figure 14(a)–(b). Comparison of predicted and measured resonance spectra for the knuckle.

Steady state dynamic analyses were also performed for the knuckle to calculate the relative magnitude of each resonant frequency. This is done by exciting the knuckle at the driver point similar to that used in the Quasar experiment around each resonant frequency. The reaction forces at the two receiver points are averaged to represent the magnitude of the forced vibration at that specific frequency. Figure 15 shows the predicted vibration magnitude at each frequency level in comparison with the experimental measurements.

Discussion

The quantitative prediction and analysis of the resonance properties of two very different parts have now been completed. The first was the connecting rod shape, which is relatively small (0.3 kg) and symmetric. The second is a typical automotive knuckle casting, which is fairly large (3 kilograms [kg]) and entirely asymmetric. These

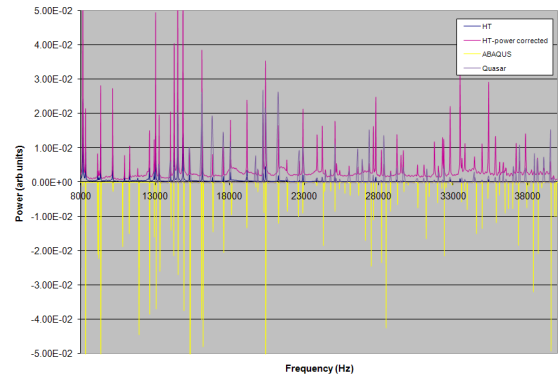


Figure 15. Comparison of steady state dynamics prediction and experimental measurements.

two cases have helped to develop a systematic procedure that puts resonance inspection on a new quantitative basis.

The relatively good resonant frequency comparison between the predicted and measured spectra for connecting rod and knuckle (as shown in Figures 6–14) indicates that experimentally measured resonances can be uniquely identified and matched to a finite element predicted mode shape.

Steady state dynamics analyses can also be used to obtain the relative response magnitude for each frequency. The discrepancies observed between the predictions and measurements are within the range allowed by the material property variations.

Two cases of mode switching are predicted around 35 kHz and 51 kHz for the connecting rod based on the FEM results. The predicted frequency gaps between the switched modes are much smaller than the measured frequency gaps, making mode switch easy to occur for a part that is slightly different from the FEM model in terms of both geometry and actual material input.

Better correlations between predictions and measurement have been achieved for the geometrically complex knuckle. For a symmetrical part such as the connecting rod, a slight deviation from the case simulated in the FEM (either in material properties or in part geometry) will lead to possible mode switch, frequency shifts and splitting of some degenerate modes due to original part symmetry. Conversely, the knuckle has more

complex surface features and no part symmetry; therefore, it will not have potentially degenerated modes to be split easily by material and geometry variation. It should be noted that the finite element predicted frequency and mode shapes also provide a basis for predicting frequency shift sensitivity of the model part to casting defects such as voids and oxide inclusions.

Conclusions

Overall, the experimental and modeling results generated to date in this study demonstrated that the modeling tools can be used to enhance the RI techniques and put RI on a quantitative basis. The overall success of the concept feasibility phase warrants the team to propose a follow-on technical feasibility study on computationally enhanced RI.

Presentations/Publications/Patents

1. C. Dasch, X. Sun, C. Lai, J. Saxton, G. Stultz, G. Palombo, C. Grupke, G. Harmon, L. Ouimet, D. Simon, and M. Jones. 2008. "Towards Quantitative Resonance Inspection: Resonance Mode Identification and Modeling." *Review of Progress in Quantitative E NDE*.
2. "NDE 701: Enhanced Resonance Inspection for Light Metal Castings." 2007. *AMD Offsite*, Southfield, MI. September 27.
3. "NDE 701: Enhanced Resonance Inspection for Light Metal Castings." 2008. *AMD Offsite*, Southfield, MI. October 29.

E. Global Quality Assessment of Joining Technology for Automotive Body-in-White

Principal Investigator: Xin Sun

Pacific Northwest National Laboratory

P.O. Box 999, Richland, WA 99352

(509) 372-6489; fax: (509) 372-6099; e-mail: xin.sun@pnl.gov

Technology Area Development Manager: Joseph A. Carpenter

(202) 586-1022; fax: (202) 586-1600; e-mail: joseph.carpenter@ee.doe.gov

Field Technical Monitor: Mark T. Smith

(509) 375-4478; fax: (509) 375-4448; e-mail: mark.smith@pnl.gov

Contractor: Pacific Northwest National Laboratory

Contract No.: DE-AC06-76RL01830

Objective

- Evaluate quantitatively the effects of missing bondline or missing welds on the global resonance signature of an automotive body-in-white (BIW).
- Assess the feasibility of a new inspection technique that will provide a global quality factor of the joining technology used for an automotive BIW.

Approach

- Evaluate the sensitivity of resonance spectroscopy to detect defects such as a partial weld or an improperly cured adhesive in a simple structure.
- Determine target values for sensitivity, reference surrogates of defects, functional requirements to be acceptable in a manufacturing environment and compatible with either inline or offline quality assurance (QA) and cost targets to ensure an inspection is economically affordable to the manufacturer.
- Determine techniques of exciting vibrational modes and other methods of stimulus that will intentionally stress a predetermined region to increase sensitivity to a selected site.
- Investigate novel means to reduce implementation cost.
- Determine advantages, technology gaps and implementation issues, investigate cost-effective means for implementation at automotive assembly plants and define paths for future development.

Accomplishments

- Fabricated spot welded samples with simple strip-like geometry: perfect and imperfect.
- Fabricated adhesively bonded samples with simple strip-like geometry: perfect and imperfect.
- Performed resonance spectroscopy measurement on both the welded and adhesively bonded samples with the Quasar system; performed resonance spectroscopy measurement on the spot-welded samples with The Modal Shop system.
- Performed preliminary finite element simulations on the natural frequencies and mode shapes for the spot-welded samples.

Future Direction

- Experimentally measure the frequency-dependent modulus for the structural adhesive used in order to perform finite element frequency extraction for the bonded samples.
- Quantify the effects of part geometric tolerance on the measured resonance spectroscopy for parts with simple geometry.
- Fabricate welded and bonded hat sections for resonance inspection (RI).
- Perform RI testing with different excitation techniques provided by different vendors.
- RI signal sensitivity study on perfect and imperfect parts.
- Perform finite element natural frequency extraction and mode shape analysis.
- Determine advantages, technology gaps, and implementation issues.

Introduction

While the domestic automotive industry continues to introduce new lightweight materials and associated joining technologies to the body-in-white (BIW), the need emerges for a global QA tool that is nondestructive and able to evaluate quickly the joining technology for an entire automotive BIW. Current practices employ statistical testing with destructive measurements that are labor intensive, ergonomically unfriendly, costly and time delayed. Further, continuous joints such as adhesive bonds or laser welds can be difficult to inspect destructively, and joints in high-strength steel can be too strong to be pried apart.

Facing these challenges, we propose to examine the concept feasibility of using a global joint quality evaluation and assurance approach by quantifying the contributions of the joint integrity (discrete as well as continuous) to the overall structural stiffness of the BIW through vibration mode and natural frequency analyses. The proposed method is computationally intensive in that it examines the BIW natural frequency and vibration modes using structural finite element analyses. Different means of structural excitation and effects of different boundary conditions will be established by detailed finite element structural/modal analyses on the BIW models provided by the original equipment manufacturers (OEMs).

Partnering with automotive manufacturers is critical to assure the techniques of straining the

BIW and performing three-dimensional (3D) imaging is conducive to a manufacturing environment and existing online production practices. Various experimental measurements including resonant spectroscopy (RS) and whole body strain measurements by techniques such as shearography (shearing speckle interferometry) will be used as experimental model validations.

The proposed techniques are capable of whole body imaging where either static or dynamic stress is applied and displacement on the order of nanometers is quantified. Comparing analyses results, the 3D displacement measurements will show a characteristic pattern when joining methods have been properly used and permit an objective means of evaluating quality.

The objective of the project is to assess the feasibility of a global inspection technique for the various joining technologies used for an automotive BIW.

Fabrication of Bonded and Welded Parts with Simple Geometry

Some 1.5 mm dual phase (DP) 980 steel sheets are used to fabricate the bonded and welded parts with simple geometry. A strip-like simple geometry is selected as the first sample geometry of this project. Two joining technologies most commonly used in an automotive BIW are used: resistance spot welding and bonding with structural adhesive. Figure 1 shows the top and bottom view of the spot welded samples with the conditions of the welds specified. The two perfect samples are

Specimen Label	Welding condition
S1 – Perfectly welded	○ ○ ○ ○ ○ ○ ○
S8 – Perfectly welded	○ ○ ○ ○ ○ ○ ○
S2 – Miss weld #1	○ ○ ○ ○ ○ ○ ○
S3 – Miss weld #2	○ ○ ○ ○ ○ ○ ○
S4 – Miss weld #3	○ ○ ○ ○ ○ ○ ○
S5 – Subsize weld #1	● ○ ○ ○ ○ ○ ○
S6 – Subsize weld #2	○ ● ○ ○ ○ ○ ○
S7 – Subsize weld #3	○ ○ ● ○ ○ ○ ○
S9 – Miss weld #4	○ ○ ○ ○ ○ ○ ○

Figure 1. Illustration of the spot welded specimens.

welded with the specified weld diameter of 6 mm. The actual weld size has been verified through metallurgical cross sectioning. Samples with sub-sized welds are labeled as poor weld and three other specimens are made with missing welds at specified locations. It should be mentioned that these welded specimens are fabricated with a regular alternating current (ac) welder under handheld condition. No sample holder or weld positioning fixture was used in the coupon fabrication process. This process will introduce some manufacturing-induced sample geometry variations in terms of weld alignment, sample edge offset and the like.

Figure 2 shows the schematic of the adhesively bonded samples with the bonding conditions illustrated. The structural adhesive Dow Betamate*73305GB is used in the bonding process. Three perfectly bonded samples are made

Specimen Label	Bonded condition
A – Perfectly bonded	████████████████████
B – Perfectly bonded	████████████████████
C – Perfectly bonded, not sanded	████████████████████
D - Missing 50mm bond line	□████████████████████
E - Missing 50mm bond line	□████████████████████
F - Missing 50mm bond line	████████████████████□
G - Missing 50mm bond line	████████████████████□
H - Missing 20mm bond line	████████████████████□
I - Missing 20mm bond line	████████████████████□

Figure 2. Illustration of the bonded samples.

and cured under vacuum condition; the rest are made with intentionally missed bond lines of 50 and 25 mm at various locations.

Resonance Spectroscopy Measurements with Quasar System

Figure 3 shows the boundary conditions used in the RI tests with the Quasar system: one point contact with Transmitter and two points contact with Receivers 1 and 2. Figure 4 shows the measured resonance signatures of the two good welded samples in the low frequency range of 0–1000 Hertz (Hz). Some similarities can be found from the resonance signatures for the two good parts, which are indicated by the blue boxes in Figure 4. The width of the blue box indicates the frequency shifts from among the two good specimens.



Figure 3. Experimental setup with the Quasar system.

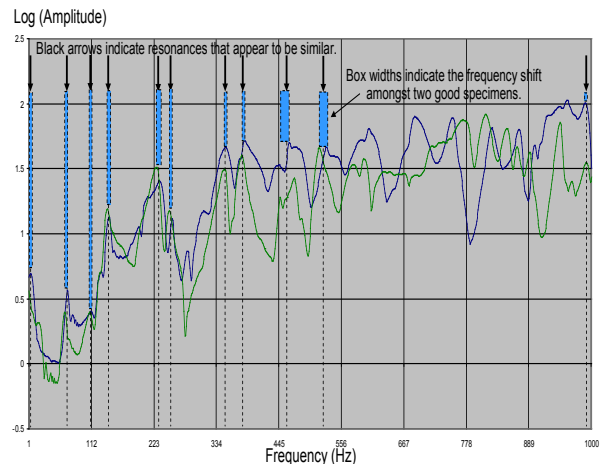


Figure 4. Measured resonance signatures of the two good welded samples: 0–1000 Hz.

Figure 5 shows the measured low frequency resonance signatures of one bad part compared with those of two good parts. Red arrows indicate the peaks for the bad part that do not match the

peaks for the two good parts. Various degrees and patterns of spectra mismatches are also obtained for the rest of the discrepant parts compared with the two good parts, similar to those shown in Figure 5.

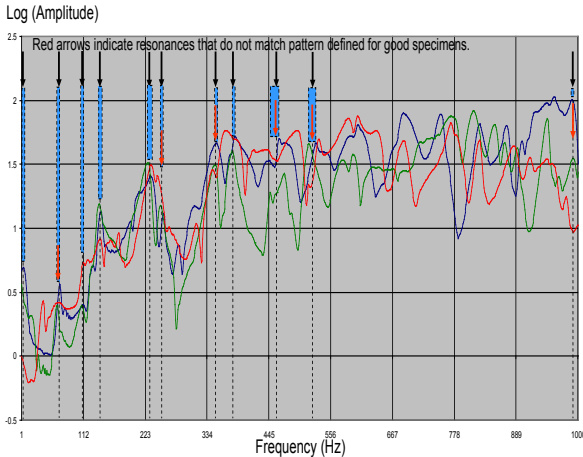


Figure 5. Comparison of resonance signatures among one bad part and two good parts.

Figure 6 shows the spectra comparison between one good part and three discrepant parts in the higher frequency range of 20–30 kilo Hz (kHz). Similar to the results in lower frequency range, noticeable frequency shifts are observed for higher frequency ranges. These results indicate that for the spot-welded samples with simple strip-like geometry, the resonance spectra show many peaks with distinguishable magnitudes. There are also detectable differences between the measured spectra for the good and discrepant parts for both

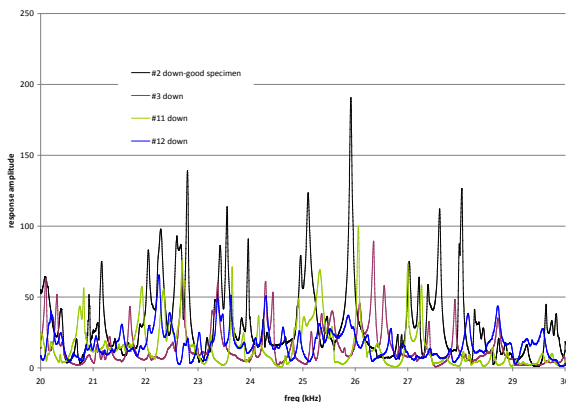


Figure 6. Comparison of resonance spectra among good and bad welded parts.

lower and higher frequencies. These results show the potential applicability in identifying missing welds and undersized welds using RI signatures/patterns.

In contrast to welded samples, the RI spectra for bonded strip-like samples do not show as much promise as those demonstrated for spot-welded samples in this preliminary stage of our work. First, RI patterns for the two perfectly bonded specimens show limited resemblance in both resonance frequencies and peak values (Figure 7). Possible reasons for the dissimilarity may be lack of consistency in line thickness between two perfectly bonded samples. Also, resonance spectra seem controlled by a global structural level resonance, with maximum peaks for most samples occurring at 17–18 kHz. Response magnitudes for all samples are in the low frequency range of 35–50 kHz due to the attenuating effect of structural adhesive. These features make it difficult for the RI technique to identify improperly bonded samples for the strip-like coupon geometry. Possible improvements to the sample design are needed.

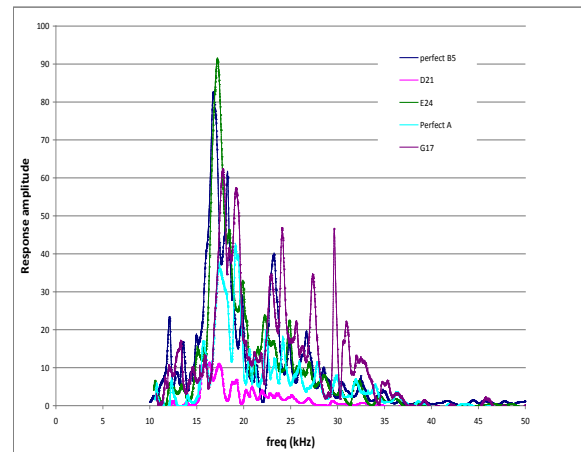


Figure 7. Comparison of resonance spectra amongst good and bad bonded parts.

Conclusions

This project received its initial funding in July 2008 and is still in initial research stages. Our next steps in this project include:

1. Fabricate small-scale hat sections using resistance spot welding and adhesive bonding on perfect and imperfect parts.
2. Obtain resonance spectra with two different RI methods (i.e., Quasar and The Modal Shop) and compare resonance spectra between perfectly and imperfectly welded/bonded parts.
3. Perform finite element natural frequency extraction and mode shape analysis on hat sections with experimentally determined frequency dependent modulus for adhesive.
4. Correlate the measured spectra with the predicted spectra for the hat sections.
5. Determine concept feasibility, technology gaps, and implementation issues for global quality assessment of joining technology for automotive BIW.